Organic & Biomolecular Chemistry

Cite this: *Org. Biomol. Chem.*, 2012, **10**, 6375

www.rsc.org/obc

PAPER

Synthesis and biological evaluation of 1,4-naphthoquinones and quinoline-5,8-diones as antimalarial and schistosomicidal agents†

Don Antoine Lanfranchi,[a] Elena Cesar-Rodo,[a] Benoît Bertrand,[a] Hsin-Hung Huang,[b] Latasha Day,[b] Laure Johann,[a] Mourad Elhabiri,[a] Katja Becker,[c] David L. Williams[b] and Elisabeth Davioud-Charvet*[a]

Received 27th April 2012, Accepted 14th June 2012
DOI: 10.1039/c2ob25812a

Improving the solubility of polysubstituted 1,4-naphthoquinone derivatives was achieved by introducing nitrogen in two different positions of the naphthoquinone core, at C-5 and at C-8 of menadione through a two-step, straightforward synthesis based on the regioselective hetero-Diels–Alder reaction. The antimalarial and the antischistosomal activities of these polysubstituted *aza*-1,4-naphthoquinone derivatives were evaluated and led to the selection of distinct compounds for antimalarial *versus* antischistosomal action. The Ag^{II}-assisted oxidative radical decarboxylation of the phenyl acetic acids using $AgNO_3$ and ammonium peroxodisulfate was modified to generate the 3-picolinyl-menadione with improved pharmacokinetic parameters, high antimalarial effects and capacity to inhibit the formation of β-hematin.

Introduction

Malaria is a mosquito-borne infectious disease caused by protozoan parasites in the genus *Plasmodium*, which is transmitted *via* the bites of infected mosquitoes. It is broadly distributed in the Sub-Saharan Africa, and tropical and sub-tropical countries worldwide. Each year, there are approximately 300 million cases of malaria, killing an estimated one million people per year, mainly infants under five years of age in Sub-Saharan Africa. Four major species of the *Plasmodium* parasite can infect humans; the most serious forms of the disease – cerebral malaria, severe anemia and death – are largely caused by *P. falciparum*. In humans, the parasites multiply first in the liver, and then infect red blood cells where they develop the symptomatic intraerythrocytic stage of the disease. If not treated, malaria can quickly become life-threatening by increasing the inflammatory environment and disrupting the oxygen supply to vital organs, such as the brain. In many parts of the world, the parasites have developed resistance to a number of malaria medicines.

Schistosomiasis is a neglected tropical disease caused by trematodes of the genus *Schistosoma*. There are five major species of *Schistosoma* infecting humans, *S. mansoni*, *S. japonicum*, *S. haematobium*, *S. intercalatum* and *S. mekongi*.

According to the World Health Organization, 200 million people are infected, 600 million people are at risk of infection and more than 200 000 deaths per year are caused by schistosomiasis. The disease is often co-endemic with malaria, found in most of Africa, Brazil, China, and the Philippines. The intermediate host of the parasite, different species of fresh-water snails, permits human infection by skin contact with infective cercariae.[1]

Our previous work on targeting redox equilibria of malaria parasites propagating in red blood cells *in vitro* and *in vivo* has led to the selection of a lead series of potent antimalarial 2-methyl-3-benzyl-1,4-naphthoquinones (benzylNQ, Fig. 1).[2]

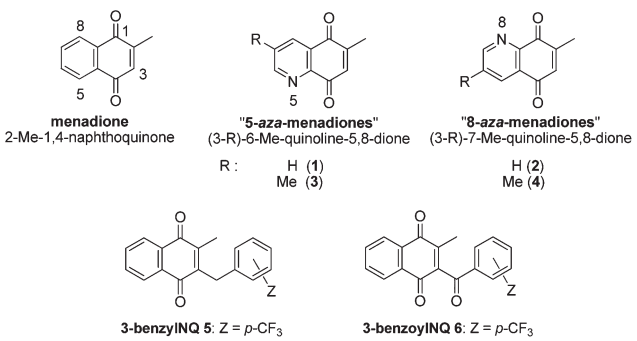

Fig. 1 Menadione and its *aza*-analogs (**1–4**), and the recently described antimalarial redox-active lead **5** and metabolite **6** derivatives.

[a]*European School of Chemistry, Polymers and Materials (ECPM) University of Strasbourg, UMR CNRS 7509, 25 Rue Becquerel, F-67087 Strasbourg, France. E-mail: elisabeth.davioud@unistra.fr; Fax: +33 (0)3 68 85 27 42; Tel: +33 3 68 85 26 20*
[b]*Department of Immunology/Microbiology, Rush University Medical Center, 1735 West Harrison Street, Chicago, IL 60612, USA*
[c]*Interdisciplinary Research Center, Nutritional Biochemistry, Justus Liebig University Giessen, Heinrich-Buff-Ring 26-32, D-35392 Giessen, Germany*

†Electronic supplementary information (ESI) available: Experimental protocols for enzymic assays and pharmacokinetics; ^1H and ^{13}C NMR spectra of compounds **1a–d**, **2a–d**, **3a–d**, **4a–d**, and **11**. See DOI: 10.1039/c2ob25812a

The antimalarial mode of action was proposed to involve a cascade of redox reactions in the parasite. The postulated bioactivation of the antimalarial 3-benzyl-menadione is thought to generate redox-active metabolites which, (i) in their oxidized form, are reduced by NADPH in glutathione reductase-catalyzed reactions within the cytosol of infected red blood cells; (ii) in their reduced forms, can convert methemoglobin(Fe^{III}), the major nutrient of the parasite, into the very slowly digestible hemoglobin(Fe^{II}).[3] Consequently, the antimalarial lead benzylNQ are suggested to perturb nutrient acquisition and the major redox homeostasis of the targeted infected red blood cells, resulting in development arrest and death of the malaria parasite at the trophozoite stage.[2a]

Of the crucial physico-chemical properties of the lead antimalarial benzylNQ that needed to be significantly improved, the solubility in aqueous solutions was the first to be targeted. One possible way to increase aqueous solubility might be to replace the naphthalene unit of the 1,4-naphthoquinone (NQ) backbone with a quinoline. Indeed, in addition to its nitrogen-solubilizing property, the quinoline moiety is frequently found in antimalarial drugs,[4] *e.g.*, chloroquine, in the 4-aminoquinoline series, quinine, in the 4-methylenealcohol quinoline series, primaquine, in the 8-aminoquinoline series, *etc*. Furthermore, the quinoline-5,8-dione core is often found in antibiotics produced by various microorganisms. These natural products are reported to exhibit a broad spectrum of biological activities including antibacterial, antifungal, antiviral, and antitumor properties.[5,6] Examples include streptonigrin, produced by an actinomycete (*Streptomyces flocculus*)[5a] lavendamycin (*Streptomyces lavendulae*),[5h,6] and quinolobactin[7] (*Pseudomonas fluorescens*) (Fig. 2).

Previous studies have highlighted the *aza*-analogs of menadione (*aza*-menadiones, Scheme 1) as substrates of both human glutathione reductase (*h*GR) and *Plasmodium falciparum* glutathione reductase (*Pf*GR).[8] Electrochemical studies showed that introduction of one nitrogen atom at C-5 or at C-8 of menadione increased the oxidant character of the molecule.[5d,8] Quinone reduction catalyzed by GR might generate one or two electrons-reduced *aza*-NQH_2 species characterized by an oxine (8-hydroxyquinoline) backbone (Fig. 2). The oxine unit is known to be a strong and selective iron (and copper) chelator.[9] This property is the feature of siderophores and contributes to the *aza*-NQ cycling between the cytosol, where quinoline-5,8-dione reduction occurs, and extracellular medium, as was illustrated with streptonigrin.[5e] Furthermore, besides its intrinsic redox cycling properties, the strong affinity for iron(III) of the oxine

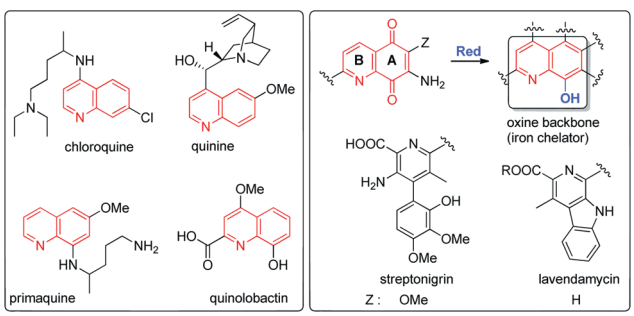

Fig. 2 Antimalarial and antibiotic drugs possessing either a quinoline, a redox-active quinoline-5,8-dione, or an oxine core.

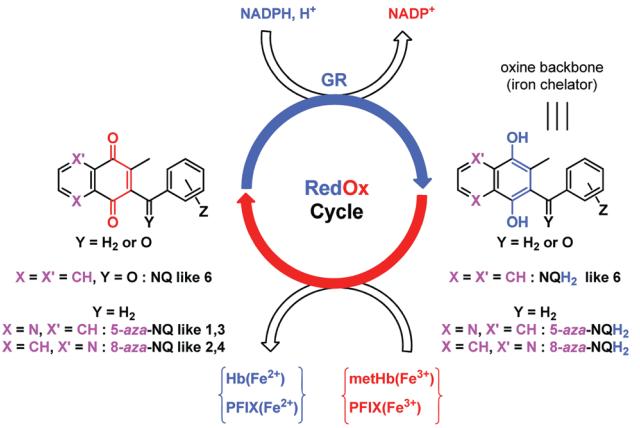

Scheme 1 General chemical structures of 1,4-naphthoquinones and related *aza*-naphthoquinones (*aza*-NQ) and bioreduction mechanism through NADPH-dependent disulfide reductase catalysis coupled to methemoglobin reduction.

chelator (log K_{LFe} = 13.69; log β_{L2Fe} = 26.3; log K_{L3Fe} = 36.9 for 8-hydroxyquinoline)[9b] was also proposed to exert an antimalarial effect.[10,11] In the present work, we considered the synthesis of the benzylated *aza*-menadiones (or the *aza*-benzylNQ) analogs, resulting from the merging of both entities – benzylNQ and *aza*-menadione – into one molecule in order to increase both the rate of the toxic redox-cycling in the parasites and the solubility of the final molecules (Scheme 1).

Results and discussion

Chemistry

The synthesis of *aza*-analogs of 3-benzylmenadiones was designed by using the very reliable Jacobsen–Torssell reaction[12] (better known as the Kochi–Anderson procedure[13]) between commercial phenylacetic acids and "*aza*-menadiones" **1–4** (quinoline-5,8-diones shown in Fig. 1). None of these quinoline-5,8-diones are commercially available; **3** and **4** are not even described compounds. Despite their relatively simple structure, these "*aza*-menadiones" are not readily synthesized in bulk.

The quinoline-5,8-dione core is usually obtained by the oxidation of 5- or 8-hydroxy/aminoquinoline derivatives as well as their 5,8-diamino, 5,8-dihydroxy, or 5,8-hydroxyaminoquinoline counterparts. Many oxidizing agents have been employed for that purpose including chromium,[14] hypervalent iodine derivatives,[15] Fremy's salt,[16] molecular oxygen and salcomine,[17] and photochemical oxidation[18] to cite a few. However, in our case, most of the appropriate 5- or 8-amino/hydroxyl or 5,8-diamino/dihydroxy/hydroxyamino (di)methylquinolines precursors are not commercially available or are very expensive, and their preparation uses a tedious route leading to poor yields.

Quinoline-5,8-diones can be synthesized in high yield (>90%) by oxidative demethylation of 5,8-dimethoxyquinolines,[19] which can be prepared from 2,5-dimethoxyaniline derivatives with the help of a modified Skraup reaction, although in poor yield (20%).[20] However, once again, the desired aniline derivatives are not commercially available.

Except for oxidative methods, the hetero-Diels–Alder reaction between an 1-*aza*-buta-1,3-diene and a 1,4-(naphtho)quinone is

an attractive method to build the quinoline-5,8-dione core.[21] Ghosez and coworkers[22] have popularized this synthetic route by adding a dimethylamino group on the *N*−1 position (acrolein *N*,*N*-dimethylhydrazone derivatives), which consequently increases the electrophilic character of the *aza*-diene. Acrolein *N*,*N*-dimethylhydrazone derivatives and quinone compounds are commercially available or are easily obtained in high yield in one or two steps.[23] Generally, the yields of hetero-Diels–Alder ranged from good to excellent. However, when applied to our substrates, the hetero-Diels–Alder reaction between bromo 2-methyl-1,4-quinones and acrolein *N*,*N*-dimethylhydrazone produced *aza*-menadiones **1** and **2** in very poor yield (only 9% and 7%, respectively).[8] In fact, it is well known that the initial *N*,*N*-dimethylhydrazine cycloadduct spontaneously releases dimethylamine that can react with the double bond of the quinonic moiety (*i.e.* hetero-Michael addition, Scheme 2, path i), giving rise to the formation of undesirable by-products and contributing to lower the yield of the hetero-Diels–Alder reaction.[23] Furthermore, dimethylamine, which can be considered as a strong base (pK_a = 10.77[24]), might react with an acidic proton to generate, for instance, a (vinyl)enolate (Scheme 2, path ii). The later might add to ketones or enones also leading to other by-products. Menadione, which possesses a vinylogous methyl ketone and an electrophilic site on its quinonic moiety, polymerizes in the presence of bases *via* quinone methide formation.[25] Moreover, amino-based compounds add on the menadione double bond or its methyl group (Scheme 2, path i & ii).[26] In this respect, the *aza*-menadione core behaves similarly.

With the aim to improve the yield of *aza*-anthraquinone synthesis, Chigr *et al.*,[25] albeit without success, added acetic anhydride as a dimethylamine scavenger during hetero-Diels–Alder between juglone (or its *O*-methyl ether) and crotonaldehyde *N*,*N*-dimethylhydrazone. In our hands, introduction of an excess of acetic anhydride (15–20 equiv) successfully led to improved yield of the *aza*-menadione **1** (43% *vs.* 7%). As a matter of fact, we observed the characteristic signals of dimethylacetamide in the ^{1}H NMR spectra of the crude mixture (Scheme 2, path b). It should be noted that both trifluoroacetic anhydride and acetyl chloride failed to substitute for acetic anhydride, leading to intractable mixture. With larger amounts of "*aza*-menadiones" **1–4** in hand, we thus performed the Jacobsen–Torssell reaction as depicted in Scheme 3. The silver(II)-mediated radical decarboxylation reaction between the four *aza*-menediones and commercial phenylacetic acids afforded sixteen targeted products (Scheme 3) in reasonably good yield (33–58% for **2a–d** and **4a–d**; 31–57% for **1a–d** and **3a–d**).

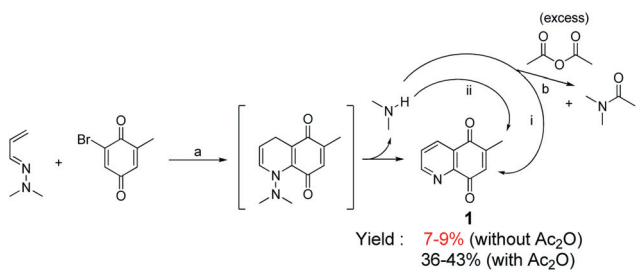

Scheme 2 Improved synthesis of the 6-methyl-quinoline-5,8-dione **1** through hetero-Diels–Alder reaction by addition of an excess of acetic anhydride. *Reagents and conditions*: (a) MeCN, rt; (b) Ac_2O excess.

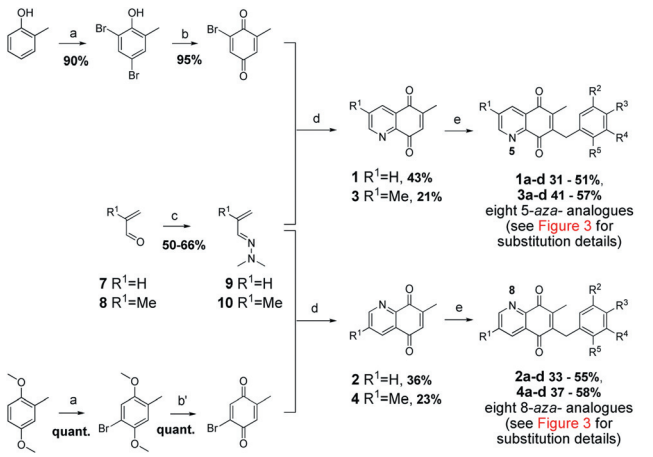

Scheme 3 Total synthesis of the *aza*-menadiones (**1–4**) and of the related 6- or 7-methyl-benzylquinoline-5,8-diones (**1a–d** to **4a–d**) in a two-step sequence. *Reagents and conditions*: (a) Br_2, AcOH, rt, 2h; (b) CrO_3, AcOH, rt, 1 h; (b′) CAN, MeCN, rt, 1 h; (c) 1,1-dimethylhydrazine, DCM, AcOH cat., 0 °C, 30 min; (d) Ac_2O, MeCN, rt, 2 h; (e) substituted phenylacetic acid, 0.35 equiv $AgNO_3$, 1.3 equiv $(NH_4)_2S_2O_8$, MeCN–H_2O (3 : 1), 85 °C, 3 h.

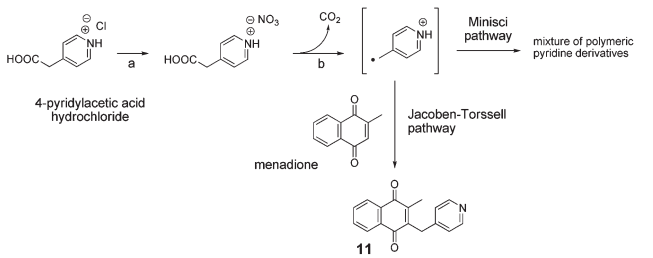

Scheme 4 Jacobsen–Torssell reaction *versus* Minisci reaction in the preparation of the picolinyl-NQ **11**. *Reagents and conditions*: (a) 1.2 equiv $AgNO_3$, 1 h; (b) menadione, 0.35 equiv $AgNO_3$, 1.3 equiv $(NH_4)_2S_2O_8$, MeCN–H_2O (3 : 1), 85 °C, 3 h.

We were also interested in introducing a nitrogen atom into the other aromatic subunit of 3-benzyl-menadiones. The first attempt to synthesize the picolinyl-NQ **11** (Scheme 4) from commercial menadione and the hydrochloride salt of 4-pyridylacetic acid under the conditions of the radical decarboxylation of Kochi–Anderson failed. As chloride anions induced precipitation of silver cation (AgCl formation) and therefore poisoned the silver catalyst, we prepared the nitrate salt of 4-pyridylacetic acid through silver counter-ion exchange (Scheme 4). The desired picolinyl-NQ **11** was obtained but with very poor yield (10%). All attempts to improve the yield failed. This was certainly due to the fact that γ-picoline radical preferred to react with itself (or the starting pyridine) rather than menadione. Indeed, there is a competition between Jacobsen–Torssell reaction (radical addition to quinone) and Minisci reaction (radical addition to pyridine).[27]

Antiparasitic activities and toxicity against human cells

All the *aza*-NQ (included the picolinyl-NQ **11**) were tested for antimalarial effects using the ^{3}H-hypoxanthine incorporation-based assay. Inhibition of the growth of *P. falciparum* by the

compounds was evaluated by determining the inhibitor concentration required for killing 50% of the parasites (IC_{50} values). In a screening assay, all compounds were tested against the CQ-resistant *P. falciparum* strain Dd2 (Table 1).

In order to gather more information about the mechanism of action of our lead compounds, we investigated the antiparasitic activity of the *aza*-menadione analogs against another blood-feeding parasite. It is well documented that both *Plasmodium* parasites and *Schistosoma* worms synthesize heme crystals similar to hemozoin (called pigment) *in vivo*.[28–30] Heme biocrystallization occurs in the gut of the worm[29a] and in the intracellular food vacuole of *Plasmodium*.[30] Both the malarial and the schistosome pigments have structures similar to synthetic β-hematin, a physicochemical feature that has been intensively reviewed.[30] Indeed, interference with hemozoin formation represents an important mechanism of the schistosomicidal action of antimalarial quinoline methanols including quinine and quinidine.[29b]

The structure–activity relationships of the *aza*-analogs were also evaluated for *S. mansoni* worm killing, assayed by visual examination of cultured worms treated with compound at 50 μM over a 48 h time course. The experiment was done under two conditions: one subset with the drug alone and another subset with the drug in the presence of human red blood cells in order to stimulate heme-catalyzed drug metabolism due to hemoglobin digestion. While the lead antimalarial 3-benzylNQ bearing a *p*-CF_3 group (**5**, Fig. 1) was very active against the malaria parasite (Table 1) with observable inhibition of the hemozoin formation in intact parasites in culture,[2a] the same compound displayed no schistosomicidal activity (Table 1). The 5-*aza*- and the 8-*aza*-analogs of **5**, **1b** and **2b** showed reduced activity against *Plasmodium* and low activity against *ex vivo* worms (Table 1).

In order to vary the substitution pattern of the benzyl moiety, the electron-withdrawing and lipophilic *p*-CF_3 group was replaced by dimethoxy groups on the benzene in 3,5 (**1c** and **2c**) or in 2,5 (**1d** and **2d**) positions (Fig. 3). Also, a methyl group was introduced at the *meta*-position to the nitrogen of the quinoline-5,8-dione core through the hetero-Diels–Alder reaction in order to observe the effect on drug metabolism. Interestingly, the 3-methyl-substituted 5-*aza* **3a–3d** provided slight potency enhancements against *Plasmodium* (Table 1) compared to the non-methylated 5-*aza*-analogs **1a–1d**, confirming methyl substitution at the *meta*-position to the nitrogen is favorable. Again, as observed with the *p*-CF_3 series, the 3-methyl-substituted 5-*aza*-

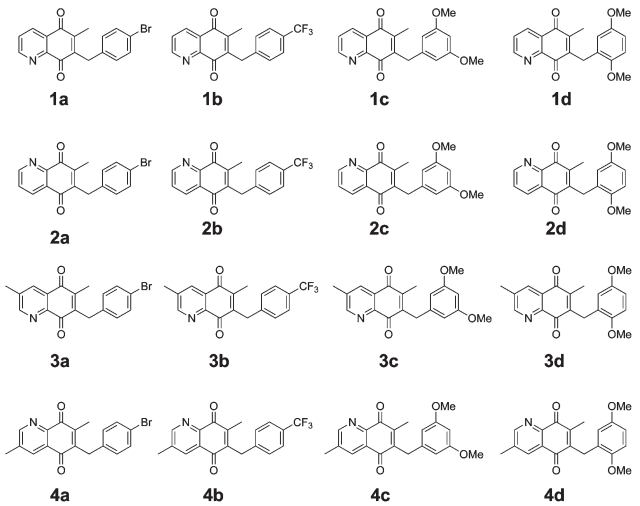

Fig. 3 Structures of the polysubstituted 6- or 7-methyl-benzylquinoline-5,8-diones (**1a–d** to **4a–d**) studied for antiparasitic action.

Table 1 Inhibition of *Schistosoma mansoni* thioredoxin-glutathione reductase, *in vitro* antimalarial and antischistosomal activities, and cytotoxicities against human cells by *aza*-analogs, the 6- or 7-methyl-benzylquinoline-5,8-diones (**1a–d** to **4a–d**), and the picoliny-NQ **11**

Compounds	*Pf* 3D7 IC_{50} (nM)	*Pf* Dd2 IC_{50} (nM)	IC_{50} (μM) or % TGR inhibition[a]	h MRC-5 toxicity IC_{50}(μM)	*Ex vivo Sm* worm killing[b] (% dead)
1a	1700–2400	2459.0	12	6.41	0% (+rbc)
1b	727	1715.0	~43% inhibition	4.45	50% (±rbc)
1c	1510.8	2172.2	3.9	2.58	50% (−rbc), < 50% (+rbc)
1d	1349.7	1206.3	~70% inhibition	5.25	<40% (±rbc)
2a	9516.6	9131.2	11.2	5.90	30% (±rbc)
2b	>3200	>3200	~48% inhibition	6.93	36% (−rbc), 41% (+rbc)
2c	>3100	>3100	~40% inhibition	2.15	68% (−rbc), 39% (+rbc)
2d	>3100	>3100	~46% inhibition	1.78	38% (−rbc), 28% (+rbc)
3a	340.25	691.3	6.02	30.05	<40% (±rbc)
3b	460.25	364.7	~58% inhibition	2.95	93% (+rbc)
3c	442.5	623.5	20.4	4.00	65% (−rbc), 43% (+rbc)
3d	391.5	437.5	~48% inhibition	1.87	71% (−rbc), 38% (+rbc)
4a	>2800	>2800	0.332	2.28	0% (+rbc)
4b	>2900	>2900	~71% inhibition	9.19	100% (+rbc)
4c	>3000	>3000	~53% inhibition	0.67	0% (+rbc)
4d	>3000	>3000	~53% inhibition	0.95	100% (+rbc)
11	119.8	109.4	~56% inhibition	3.12	0% (±rbc)
5	67.5	69.2	~69% inhibition	>32[2a]	0%[c]
Chloroquine	7.9	147.7	~33% inhibition	51.54[2a]	0%[c]

[a] Data were measured in the DTNB reduction assay in 0.1 M phosphate buffer, 10 mM EDTA at 25° C, in the presence of 100 μM NADPH, 10 nM *Sm*TGR and 50 μM compound. [b] Data represent the results from three separate experiments carried out at 50 μM drug concentration in the presence or in the absence of red blood cells (rbc). Data were collected by visual examination of worm movement and shape. [c] +10 μM human hemoglobin after 24 h.

3c, **3d** and 8-*aza*-analogs **4b**, **4d** can decrease *S. mansoni* worm survival significantly compared to the non-methylated 5-*aza*-**1a–1d**, and 8-*aza*-analogs **2a–2d**. Likewise, the *p*-CF_3 group was also replaced by *p*-Br. No improvement in antiplasmodial or antischistosomal activity was noted.

The picolinyl-NQ **11** was found to be slightly less active than the lead **5** against both *P. falciparum* strains in culture, but both were ineffective as *S. mansoni* worm killing agents no matter whether red blood cells were present or not. The results detailed in Table 1 showed clear evidence that we can dissociate the antimalarial activity from the worm killing capacity by introduction of the structural diversity at the benzyl chain or/and at the quinoline ring of the quinoline-5,8-dione core.

In conclusion, all 5-*aza*- and the 8-*aza*-menadione analogs had reduced activity against *Plasmodium* and minimal ability to kill *ex vivo* worms at 50 μM. However, from the structure–activity relationships, significant enhancements or decreases in the antiparasitic activities could be drawn.

Enzymatic assays

In a previous work, we investigated the redox-cycling capacity and the inhibitory effects of a series of six 5-*aza*- and 8-*aza*-menadiones on three disulfide reductases, *i.e.* the human glutathione reductase and both human and *Plasmodium falciparum* thioredoxin reductases (TrxR).[8] In the present study, all compounds from the 5-*aza*- and 8-*aza*-menadione series were evaluated for their potential to inhibit *S. mansoni* thioredoxin glutathione reductase (*Sm*TGR), a hybrid enzyme that carries out both thioredoxin and glutathione reduction in the worm,[31] in the disulfide reduction assay using the artificial substrate DTNB. A primary screening *Sm*TGR assay was carried with each compound at 50 μM. Compounds inhibiting the enzyme by ≥80% were further analyzed. The results of this study are presented in Table 1. Among all the 5-*aza*-menadione and 8-*aza*-menadione derivatives tested, only six compounds inhibited *Sm*TGR by ≥80%; the remaining inhibited the enzyme by 40 to 70%. The compounds with the most potent *Sm*TGR inhibitory activities are **11**, **1a**, **1c**, **3a**, **3c**, **4a**, and **2a**. Most of these compounds displayed moderate *Sm*TGR activities with IC_{50} values from 3.9 to 20.4 μM. However, **4a** displayed a very potent *Sm*TGR inhibitory activity in the nanomolar range with an IC_{50} value of 332 nM. There was however, no correlation between *Sm*TGR inhibition and worm killing activity. This is possibly due to the fact that *Sm*TGR interaction with the quinones was investigated through inhibition of disulfide reduction in this study. It is well documented that many flavin-binding disulfide reductases show diaphorase activities catalyzing the reduction by NAD(P)H of various dyes (*e.g.* methylene blue) and quinones which act as hydrogen acceptors. Menadione reduction was not always correlated to inhibition of disulfide reduction, as illustrated with *P. falciparum* glutathione reductase[2a,32a] *vs. Trypanosoma cruzi* dihydrolipoamide dehydrogenase (LipDH).[33a] The latter flavoenzyme, previously called menadione reductase, did not exhibit high and significant decreased disulfide reductase activity in the presence of menadione and analogs.[33b] The flow of electrons from the nicotinamide ring of NADPH proceeds *via* the flavin ring of GR-bound FAD to menadione.[32b] The substrate capacity of our *aza*-menadione derivatives was exemplified in the following GR assays, by investigating metHb reduction, in the presence of the picolinyl-NQ **11**, and the NADPH-GR system.

Finally, the toxicity of all *aza*-1,4-naphthoquinone derivatives was evaluated against the human lung fibroblast cell line MRC-5. Compared to the starting lead compound **5** which had low toxicity against two human cell lines, the 5-*aza*- and the 8-*aza*-analogs exhibited low IC_{50} values, suggesting modification of the partition coefficient of final *aza*-molecules may have increased their cell penetration capabilities. Another explanation could also come from the modified redox potential values[8] impacting the specificity of the subversive substrates with respect to the diaphorase activities of a larger panel of flavoenzymes from the host, *e.g.* human TrxR or LipDH. The least toxic compound, **3a**, was found to be the 3-methyl-5-*aza*-analog of the potent lead antimalarial benzylNQ with a *p*-Br-substitution at the benzyl chain. The structure–activity relationships and the rather low molecular weight of the lead benzylNQ **5** (~300 Da) suggest that there is a 'room' for varying the chemical modification of aromatic rings to modulate antiparasitic action *vs.* specificity to the targets *vs.* redox potentials *vs.* cytotoxicity against human cells.

Physico-(bio)chemical assays

In this preliminary physico-(bio)chemical study, we evaluated the strength of the interactions between the picolinyl-NQ **11** and iron(III)-containing targets (hematin, methemoglobin) in solution under quasi-physiological conditions. *Plasmodium* (acidic food vacuole) and *Schistosoma* (gut of the worm[29]) parasites digest methemoglobin (metHb), resulting from endogenous oxidation of hemoglobin (Hb), as a source of essential nutrients. Both parasites neutralize these toxic heme species *via* major detoxification processes, mainly in the food vacuole at pH 5.2 where autoxidation of hemoglobin(Fe^{II}) takes place: (i) biocrystallization into an insoluble and "inert" crystal called hemozoin[29,30] (malaria pigment or *Schistosoma* pigment), (ii) rapid peroxidative decomposition by reacting with H_2O_2,[34] and in the cytosol (iii) activities of an efficient thiol redox network based on the regeneration of thiols catalyzed by NADPH-dependent disulfide reductases (GR of *Plasmodium*-infected human erythrocytes and *Schistosoma* TGR).[2,31,35,36] Several series of antimalarial drugs have been reported to exert their effects through the enhancement of free heme toxicity *via* the inhibition of hemozoin formation (*e.g.* 4-aminoquinolines,[4,30,37] quinoline methanols,[29c,38] endoperoxides[39] or xanthones[40]).

Inhibition of hemozoin formation represents the most important rational drug development strategy for malaria over the last few years.[4,30] In this context, the ability of a heme binding agent to strongly interact with heme in solution is usually an important pre-requisite for further development. Fig. 4A shows the spectrophotometric titration of hematin binding by picolinyl-NQ **11** by monitoring changes in absorption of the hematin π–π dimer.[30d,41] Concomitant bathochromic shifts and narrowing of the Soret band were observed indicating the formation of complexes of picolinyl-NQ **11** with hematin (Fig. 4B). An apparent dissociation constant (K_D = 1.66 μM) and the stoichiometry of the species formed at equilibrium ([$(Fe^{III}PPIX)_2$(L)] with log β_{21}

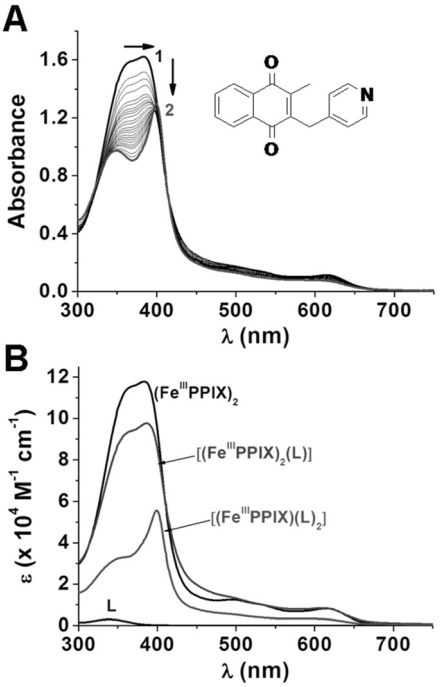

Fig. 4 (**A**) Absorption spectrophotometric titration of hematin (in a π–π dimeric state) by the picolinyl-NQ **11** (noted L). Solvent: 0.2 M HEPES buffer pH 7.5; l = 1 cm; $[Fe^{III}PPIX]_{tot}$ = 2.93 × 10^{-5} M. In panel A, spectra were recorded at varying $[L]_{tot}/[Fe^{III}PPIX]_{tot}$ ratio, (1) from $[L]_{tot}/[Fe^{III}PPIX]_{tot}$ = 0 to (2) $[L]_{tot}/[Fe^{III}PPIX]_{tot}$ = 2.44. (**B**) Absorption electronic spectra of the complexes formed between Fe^{III}PPIX and the picolinyl-NQ **11** ligand.

= 12.6 ± 0.2 and $[Fe^{III}PPIX)(L)_2]$ with log β_{12} = 10.6 ± 0.2) have been determined.

After evaluation of the heme binding capacities of picolinyl-NQ **11**, we undertook a biochemical investigation[42] of the activity of this compound to inhibit hematin crystallization to β-hematin (*i.e.* synthetic equivalent of hemozoin). This assay, performed at pH ~ 5 (*i.e.*, pH at which hemozoin biomineralization efficiently occurs), is based on a classical hematin quantification method.[43] An IC_{50} value of 4.3 (Drug (equiv)/Hematin (equiv)) with ~80% of inhibition of β-hematin formation by the picolinyl-NQ **11** was obtained (Fig. 5). Taken together, these preliminary data clearly illustrate that the heme binding properties observed for the picolinyl-NQ **11** may account for its capacity to efficiently prevent β-hematin formation *in vitro* and to a significant extent of hemozoin formation *in vivo*.

As exemplified with our antimalarial lead 3-benzylmenadione derivatives and with methylene blue by Schirmer's group,[41a,44] the redox-based mechanism of action against malarial parasites is a recent molecular therapeutic strategy to cure parasitic diseases.[2,41] Efficient and fast reduction of methemoglobin(Fe^{III}) to oxyhemoglobin(Fe^{II}) through continuous use of a NADPH flux under catalysis of disulfide reductases (GR or TGR) in the presence of redox-active mediators (naphthoquinones,[2] *aza*-naphthoquinones[8]) is expected to significantly slow down metHb(Fe^{III}) digestion. We therefore investigated the ability of the picolinyl-NQ **11** to inhibit β-hematin formation, not solely on the basis of hematin binding (Fig. 5), but also on the basis of electron transfer reactions. We evaluated if, in its reduced states, the picolinyl-

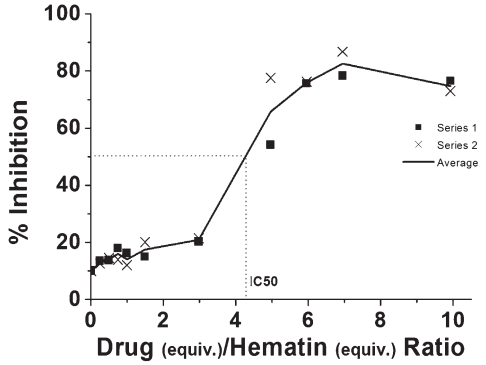

Fig. 5 Inhibition of β-hematin crystallization by the picolinyl-NQ **11** at pH 4.5 (12.9 M acetate buffer) measured by UV-visible absorption spectrophotometry using pyridine (5% by volume) as reporting reagent. (solvent: water; pH 7.5 HEPES buffer 200 mM then 20 mM, T = 25 °C). The cross (×) and the square (■) labels correspond to two independent replicate, while the solid line corresponds to the averaged values.

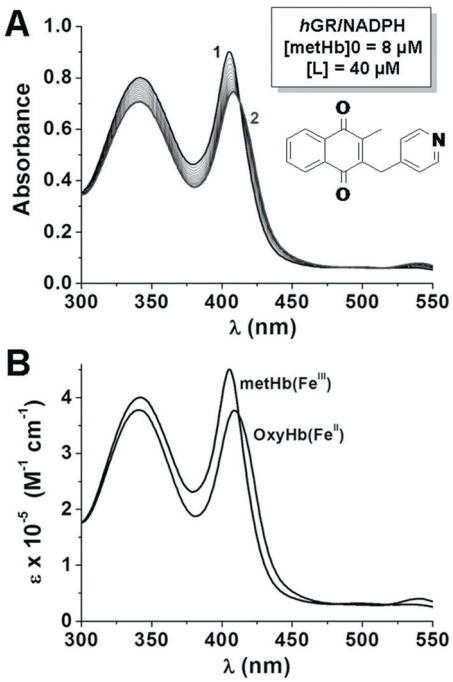

Fig. 6 (**A**) UV-visible absorption spectra recorded as a function of time showing the fast metHb(Fe^{III}) Reduction in the coupled assay with the *h*GR/NADPH system in the presence of the picolinyl-NQ **11**. (**B**) Electronic spectra of the reactants and the products of the metHb(Fe^{III}) reduction. Solvent: water (*h*GR acetate buffer pH 6.9 + 47 mM K_2PO_4 + 200 mM KCl); T = 37.0 °C; 40 µM NADPH + 133 nM *h*GR + 8 µM metHb + 40 µM picolinyl-NQ **11**. In panels A and B, spectra were recorded as a function of time (1) at t = 0; (2) at t ~ 18 min.

NQ **11** can trigger metHb(Fe^{III}) reduction to oxyHb(Fe^{II}) (Fig. 6).

The picolinyl-NQ **11** is efficiently reduced by NADPH with mediation of GR and, in its reduced forms (semi-naphthoquinone or dihydronaphthoquinone), catalytically and specifically, transfers electrons to methemoglobin(Fe^{III}) (k^{obs}_{red} = (1.95 ±

0.02) × 10^{-3} s^{-1}). Both events, oxidizing the reductants (like NADPH) and reducing the oxidants (like Fe(III)-containing targets), in a continuous redox cycle are expected to lead to the death of the parasites. It appeared from our physico-(bio)chemical investigations that the capacity of the reduced picolinyl-NQ **11** to rapidly and efficiently reduce metHb has also to be taken into account to rationalize their potential in inhibiting (directly or indirectly) hemozoin formation.

Pharmacokinetics

At the lead discovery stage, it is critical that the compounds identified are not only optimized for their efficacy against the selected parasites but also to have a characteristic "drug profile". This is essential for successful downstream development; the criteria include limited and tolerable side effects, high oral bioavailability, and an appropriate pharmacokinetic pattern.[45] When synthesizing a library of naphthoquinone derivatives we were further interested in determining if quinoline-5,8-dione core scaffold has suitable properties for oral bioavailability by simply analyzing the structural physicochemical properties (*e.g.* number of hydrogen bonding partners, MW, log *D*) according to the Lipinski *et al.*'s rule, which referred to simple descriptors correlated to oral drug absorption.[45] Thus, determination of the solubility (in μM), lipophilicity index (CHI, Chromatographic Hydrophobicity Index), and log *D* were determined in order to predict suitability of the compounds for oral drug administration. In addition, potential increases in resistance to drug metabolism were introduced through the hetero-Diels–alder reactions by preparing a series of metabolically-resistant *aza*-analogues through the introduction of a methyl group with respect to the nitrogen in the phenyl rings of the 3-benzylNQ core. The results of these profiles are shown in Table 2.

The lead 3-benzylmenadione **5**, with the *p*-CF_3 group, has very low solubility in water. Introduction of the nitrogen at the phenyl rings of the 3-benzyl-NQ core slightly increased the solubility of the final quinoline-5,8-diones. The most soluble compound was the menadione substituted at C-3 by a 4-picolinyl chain (see derivative **11**). Beyond solubility profiling, the *aza*-analogues displayed significantly lower lipophilicities and log *D* values, a positive feature for improving the antimalarial drug candidates. However, with this and other series of compounds, we observed that antischistosomal molecules required a minimal lipophilicity, probably because the lipid-rich tegument enveloping the worm is an effective barrier to most hydrophilic molecules.

Table 2 Solubility and selected ADME properties[a] of the lead benzylNQ and representative *aza*-analogs

Compound	CHI[b]	log $D_{7.4}$	Solubility (μM)
5	115	4.68	0 (nd)[c]
4b	96	3.68	0.29 ± 0.01
3b	96	3.68	0.08 ± 0.01
3a	96	3.71	0.03 ± 0.00
1a	90	3.37	1.09 ± 0.02
11	76	2.68	0.29

[a] Protocols for measurements are given in ESI. [b] CHI (chromatographic hydrophobicity index).[c] nd: not detected.

Discussion

Malaria and schistosomiasis-associated pathologies are respectively caused by the continuous expansion of *Plasmodium* parasites inside host erythrocytes, and to egg-laying by adult worms living in the host bloodstream. Both parasites, the protozoan *Plasmodium* and the helminth *Schistosoma*, feed on host hemoglobin. This process along with the immune response of the host toward infection causes an intense flux of reactive oxygen species. To maintain a reducing intracellular milieu in oxygen-rich environments, malaria and schistosome parasites have evolved a complex antioxidative network based on two central electron donors, glutathione and thioredoxin, that are regenerated by NADPH-dependent disulfide reductases. *Plasmodium berghei* GR and thioredoxin reductase are dispensable flavoenzymes for proliferation of the pathogenic blood stages, but GR-null malaria parasites, with normal blood stage growth, arrest during development in the mosquito.[46] As clearly demonstrated, GR is vital for extracellular parasite development inside the insect vector, whereas thioredoxin reductase is dispensable during the entire parasite life cycle. By comparison, *Schistosoma* worms have a unique multifunctional NADPH-dependent enzyme, TGR, which is essential to maintain a proper redox homeostasis during its survival in the host; the requirement of TGR was assessed by inhibitor studies and RNA interference experiments.[31b] These findings corroborate our drug design projects based on the development of subversive substrates of GR[2,26,32c,41a] and TGR[31b] combined with the inhibition of hemozoin formation – two drug targets selected for many years as promising antimalarial and antischistosomal intervention strategies.

In the malaria *P. berghei* blood stage parasite, even if GR and TrxR are able to largely compensate for each other, the simultaneous interference of both human erythrocytic and *Plasmodium* GR by redox-active agents is expected to lower the NADPH flux in infected red blood cells. Two successful examples of "multi-target-directed redox-cyclers" are illustrated with the potent antiplasmodial agents, methylene blue and the 3-benzyl menadiones, acting as human and plasmodial GR redox-cycling substrates in infected red blood cells. Simultaneously interfering with redox metabolism by distinct disulfide reductases and hemoglobin catabolism/heme detoxification represents a promising approach to antimalarial drug development. As demonstrated with fluorine-based suicide substrates of GR[2a,32b] the bioactivation of the antimalarial benzylNQ appeared to be essential to observe the antimalarial effects of the lead series. The objective was not exclusively to inhibit GSSG reduction in infected red blood cells because, from biochemical[47] and molecular biology studies,[46] GSSG reduction can be maintained by other redox partners of the thiol network, *e.g.* reduced thioredoxin. Of greater importance is the NADPH flux, which can be diverted to a futile cycle in the presence of redox-active agents by exploiting the GR reductive catalysis for drug bioactivation in infected red blood cells and/or drug combination in concert with metHb catabolism.[2,41] As reported earlier, the high frequency of the sickle-cell hemoglobinopathy and of glucose-6-

phosphate dehydrogenase (G6PD) enzyme deficiency in malaria endemic regions is believed to be due to a natural genetic protection against fatal malaria.[48] Indeed, numerous hemoglobinopathies, G6PD and GR deficiencies have been shown to result in decreased half-life of red blood cells, due to their enhanced phagocytosis and rapid elimination from the bloodstream by the immune system.[49] At the biochemical level, these genetic variations result in protection from severe malaria due to a decreased flux of NADPH and increased oxidative stress in the erythrocytes, making the intracellular milieu hostile for the survival of *Plasmodium*.

Our studies with redox-active agents displaying potent antimalarial action should be continued by investigation of the mechanism of interaction of these compounds in the full parasitic cycle, in particular with *Plasmodium* GR in mosquito stages. These studies on optimization of lead antimalarial benzylNQ demonstrated the tremendous work which remains to be done, likely because the excellent antimalarial action of the lead benzylNQ might result from subtle combination of pharmacokinetics parameters and interference with different targets in *Plasmodium* infecting the human and insect hosts: GR catalysis, metHb reduction, drug transport, hematin complex formation, *etc.* For schistosomiasis, the "multi-target-directed redox-cycler" approach is directly focused on one sole protein, TGR, which represents the "bottleneck" of the redox thiol network in *Schistosoma mansoni* worms.[31b] Although both parasites feed on hemoglobin, the biology of multicellular *Schistosoma* worms is significantly distinct from that of unicellular *Plasmodium*: the presence of highly lipophilic tegument enveloping the worm *vs.* a complex vesicular system that extends from the parasitophorous vacuole into *Plasmodium*-infected red blood cell cytoplasm and the plasma membrane; presence of a gut *vs.* a food vacuole for hemoglobin digestion, *etc*… The present work is a first step in the development of redox-active agents against blood-feeding malaria and schistosome parasites.

Conclusion

Taken together, the available data suggest that improving the pharmacokinetic properties of our lead compounds need to address different parameters to facilitate future drug development: (i) regioselective introduction of structural elements (nitrogen, methyl groups) in the aromatic ring of menadione was achieved by developing a two step-synthesis of 1,4-naphthoquinones by hetero-Diels–Alder reactions; (ii) increasing the solubility/decreasing the lipophilicity of our compounds was accomplished by introduction of nitrogen to the phenyl ring of the lead benzylNQ, which however increased the cytotoxicity against the human cells; (iii) introduction of CF_3 and methyl groups and a nitrogen atom resulted in differential antimalarial *vs.* antischistosomal activities of compounds and introduction of a methyl group in *meta*- to the nitrogen increased the antiparasitic action; (iv) the presence of the pyridine, at the picolinyl- *vs.* benzyl-chain increased the binding to hematin, and β-hematin formation inhibition. Increasing the structural diversity within the series of benzylNQs might allow for the development of compounds exclusively targeting either malaria or schistosomes parasites. This goal was partially achieved with compounds such as **4b** which specifically kills 100% of *S. mansoni* worms, and **11** which, by contrast, is devoid of antischistosomal activity but possess good antimalarial activity (Table 1). Future studies will be aimed at metabolically blocking key sites of unproductive metabolism and modulating lipophilicity and solubility to improve the pharmacokinetics of the lead compounds while still maintaining similar oxidant character and specific antiparasitic potency.

Experimental

Chemistry

Melting points were determined on a Büchi melting point apparatus and were not corrected, the solvent from which compounds were crystallized is indicated in brackets. ^{1}H (300 MHz) and ^{13}C (75 MHz) NMR spectra were recorded on a Bruker DRX-300 spectrometer, chemical shifts were expressed in ppm relative to TMS; multiplicity is indicated as s (singlet), d (doublet), t (triplet), q (quadruplet) and m (multiplet). Elemental analyses were carried out at the Mikroanalytisches Laboratorium der Chemischen Instituteder Universität Heidelberg. EI MS were recorded at facilities of the Institut für Organische Chemie der Universität Heidelberg. Analytical TLC was carried out on precoated Sil G-25 UV_{254} plates from Macherey Nagel. Flash chromatography was performed using silica gel G60 (230–400 mesh) from Macherey Nagel. Starting materials 6-methylquinoline-5,8-dione **1** and 7-methylquinoline-5,8-dione **2**, were synthesized according to reported procedures,[8] but with introduction of an excess of acetic anhydride (15–20 equiv) prior to addition of the starting quinone dropwise to the azadiene.

3,6-Dimethylquinoline-5,8-dione 3. 1,1-Dimethyl-2-(2-methylallylidene)hydrazine (2.17 g, 19.37 mmol, 1.3 equiv) was added in 245 mL of MeCN followed by acetic anhydride (19 mL). The reaction mixture was stirred at room temperature. 2-bromo-6-methylcyclohexa-2,5-diene-1,4-dione (3.00 g, 14.9 mmol, 1 equiv) in 85 mL of MeCN was then added dropwise (slowly during 80 min). The reaction mixture was stirred at room temperature during 120 min. The crude was then concentrated and purified by column chromatography using diethyl ether and toluene (70 : 30) to give a brown solid. Yield: 21%; mp: 165 °C dec. (from Et_2O). δ_H (300 MHz, $CDCl_3$, Me_4Si) 8.86–8.87 (d, ^4J = 1.7 Hz, 1H), 8.2 (d, ^4J = 2 Hz, 1H), 6.91 (d, ^4J = 1.5 Hz, 1H), 2.54 (s, 3H), 2.28–2.29 (d, ^4J = 1.5 Hz, 3H) ppm. δ_C (75 MHz, $CDCl_3$, Me_4Si) 185.33 (C═O), 183.35 (C═O), 155.14 (CH), 147.64 (C_q), 145.63 (C_q), 138.51 (C_q), 136.09 (CH), 134.32 (CH), 128.74 (C_q), 18.88 (CH_3), 16.28 (CH_3) ppm. EIMS (70 eV) *m/z*: 187.0 ($[M]^+$, 100). Elemental analysis $C_{11}H_9NO_2$: calc: C, 70.58; H, 4.85; N, 7.48. Found: C, 70.40; H, 5.93; N, 7.37.

3,7-Dimethylquinoline-5,8-dione 4. The title compound was prepared in the same manner as **3** but from 2-bromo-5-methylcyclohexa-2,5-diene-1,4-dione. Yield: 23%; mp: 150–151 °C (from Et_2O). δ_H (300 MHz, $CDCl_3$, Me_4Si) 8.85 (s, 1H), 8.22 (s, 1H), 6.97–6.98 (d, ^4J = 1.5 Hz, 1H), 2.53 (s, 3H), 2.22–2.23 (d, ^4J = 1.5 Hz, 3H).δ_C (75 MHz, $CDCl_3$, Me_4Si) 184.56 (C═O), 183.68 (C═O), 155.09 (CH), 149.04 (C_q), 145.63 (C_q), 138.65 (C_q), 134.86 (CH), 133.94 (CH), 128.67 (C_q), 18.86 (CH_3),

16.69 (CH_3). EIMS (70 eV) *m/z*: 187.0 ($[M]^+$, 100). Elemental analysis $C_{11}H_9NO_2$: calc: C, 70.58; H, 4.85; N, 7.48. Found: C, 70.35; H, 5.03; N, 7.28.

General procedure for synthesis of the related 6- or 7-methyl-benzylquinoline-5,8-dione derivatives (1a–d to 4a–d). One of the four *aza*-menadiones, (**1–4**) (1 equiv, 0.05 mmol mL^{-1}) and a substituted phenyl acetic acid derivative (2 equiv) were added to a stirred solution of MeCN–H_2O (3 : 1) and heated at 85 °C (70 °C in the flask). $AgNO_3$ (0.25 equiv) was added first and then $(NH_4)_2S_2O_8$ (1.3 equiv, 0.36 mmol mL^{-1}) in MeCN–H_2O (3 : 1) was added dropwise. The reaction mixture was additionally heated for 2–3 h at 85 °C. MeCN was evaporated and the mixture was extracted with dichloromethane. The crude mixture was purified by flash chromatography on silica gel using a mixture diethyl ether and toluene (70 : 30). When necessary, the final 6- or 7-methyl-benzylquinoline-5,8-dione (**1a–d to 4a–d**) was further purified by trituration in diethyl ether.

7-(4-Bromobenzyl)-6-methylquinoline-5,8-dione 1a. Yield: 46%; mp: 132–133 °C (from Et_2O). δ_H (300 MHz, $CDCl_3$, Me_4Si) 9.01 (dd, J = 4.6 Hz, 1.7 Hz, 1H), 8.41 (dd, J = 7.9 Hz, 1.7 Hz, 1H), 7.65 (dd, J = 7.9 Hz, 4.6 Hz, 1H), 7.24 ($(AB)_2$ system, J = 8.4 Hz, $\Delta\nu$ = 114.9 Hz, 4H), 3.99 (s, 2H), 2.32 (s, 3H) ppm. δ_C (75 MHz, $CDCl_3$, Me_4Si) 184.0 (C═O), 183.5 (C═O), 154.5 (CH), 147.5 (C_q), 145.5 (C_q), 144.3 (C_q), 136.5 (C_q), 134.6 (CH), 131.8 (2 × CH), 130.2 (2 × CH), 128.7 (C_q), 127.5 (CH), 120.5 (C_q), 31.9 (CH_2), 13.5 (CH_3) ppm. EIMS (70 eV) *m/z*: 342.9 (22) $[M + H]^+$, 327.9 (92), 325.9 (100), 247.1 (47). Elemental analysis $C_{17}H_{12}BrNO_2$: calc: C 59.67, H 3.53, N 4.09, Br 23.35. Found C 59.56, H 3.68, N 4.18, Br 23.50.

7-(4-(Trifluoromethyl)benzyl)-6-methylquinoline-5,8-dione 1b. Yield: 51%; mp: 124–126 °C (from Et_2O). δ_H (300 MHz, $CDCl_3$, Me_4Si) 9.03 (dd, J = 4.7 Hz, 1.8 Hz, 1H), 8.43 (dd, J = 7.9 Hz, 1.8 Hz, 1H), 7.67 (dd, J = 7.9 Hz, 4.7 Hz, 1H), 7.44 ($(AB)_2$ system, J = 8.0 Hz, $\Delta\nu$ = 56.4 Hz, 4H), 4.11 (s, 2H), 2.34 (s, 3H) ppm. δ_C (75 MHz, $CDCl_3$, Me_4Si) 184.0 (C═O), 183.5 (C═O), 154.6 (CH), 147.5 (C_q), 145.9 (C_q), 144.0 (C_q), 134.7 (CH), 129.0 (q, J = 33.7 Hz, C_q), 128.9, (CH), 128.7 (C_q), 127.6 (CH), 125.7 (q, J = 3.7 Hz, 2 × CH); 122.2 (C_q), 32.3 (CH_2), 13.7 (CH_3) ppm. EIMS (70 eV) *m/z*: 331.0 ($[M]^+$, 23), 316.0 ($[M–CH_3]^+$, 100). Elemental analysis $C_{18}H_{12}F_3O_2 \cdot 0.3H_2O$: calc: C, H 3.53, N 4.09, Br 23.35. Found C 59.56, H 3.68, N 4.18.

7-(3,5-Dimethoxybenzyl)-6-methylquinoline-5,8-dione 1c. Yield: 31%; mp: 152–153 °C (from Et_2O). δ_H (300 MHz, $CDCl_3$, Me_4Si) 9.02 (dd, J = 4.7 Hz, J = 1.6 Hz, 1H), 8.43 (d, ^3J = 7.7 Hz, J = 1.6 Hz, 1H), 7.66 (dd, J = 7.7 Hz, ^4J = 4.7 Hz, 1H), 6.37–6.30 (m, 3H), 4.00 (s, 2H), 3.75 (s, 6H), δ = 2.33 (s, 3H) ppm. δ_C (75 MHz, $CDCl_3$, Me_4Si) 184.0 (C═O), 183.6 (C═O), 160.9 (C_q), 154.3 (CH), 147.6 (C_q), 145.7 (C_q), 144.6 (C_q), 139.7 (C_q), 134.7 (CH), 128.9 (C_q), 127.5 (CH), 106.8 (2 × CH), 98.1 (CH), 55.3 (2 × OCH_3), 32.5 (CH_2), 13.6 (CH_3) ppm. EIMS (70 eV) *m/z*: 323.1 ($[M]^+$, 69), 308.1 ($[M–CH_3]^+$, 88), 77.1 (100). Elemental analysis $C_{19}H_{17}NO_4$: calc: C, 70.58; H, 5.30; N, 4.33. Found: C, 70.56; H, 5.37; N, 4.21.

7-(2,5-Dimethoxybenzyl)-6-methylquinoline-5,8-dione 1d. Yield: 48%; mp: 122–123 °C (from Et_2O). δ_H (300 MHz, $CDCl_3$, Me_4Si) 9.02 (d, ^3J = 4.5 Hz, 1H), 8.43 (d, ^3J = 7.8 Hz, 1H), 7.66 (dd, ^3J = 7.8 Hz, ^3J = 4.5 Hz, 1H),: 6.72 (m, 3H), 4.01 (s, 2H), 3.78 (s, 3H), 3.71 (s, 3H), 2.26 (s, 3H) ppm. δ_C (75 MHz, $CDCl_3$, Me_4Si) 183.9 (C═O), 183.6 (C═O), 154.1 (CH), 153.5 (C_q), 151.5 (C_q), 147.5 (C_q), 145.9 (C_q), 145.1 (C_q), 134.7 (CH), 129.0 (C_q), 127.4 (CH), 127.0 (C_q), 116.4 (CH), 111.2 (CH), 111.1 (CH), 55.9 (CH_3), 55.6 (CH_3), 27.0 (CH_2), 13.3 (CH_3) ppm. EIMS (70 eV) *m/z*: 324.1 ($[M + H]^+$, 24), 323.1 ($[M]^+$, 100); 308.1($[M–CH_3]^+$, 54). Elemental analysis $C_{19}H_{17}NO_4$: calc: C, 70.58; H 5.30; N, 4.33. Found: C, 70.51; H, 5.38; N, 4.22.

6-(4-Bromobenzyl)-7-methylquinoline-5,8-dione 2a. Yield: 33%; mp: 105–106 °C (from Et_2O). δ_H (300 MHz, $CDCl_3$, Me_4Si) 9.02 (s, 1H), 8.43 (d, J = 7.5 Hz, 1H), 7.64–7.66 (d, J = 6.1 Hz, 1H), 7.26 ($(AB)_2$ system, J = 8.3 Hz, $\Delta\nu$ = 72.4 Hz, 4H), 4.05 (s, 2H), 2.27 (s, 3H) ppm. δ_C (75 MHz, $CDCl_3$, Me_4Si) 184.7 (C═O), 183.0 (C═O), 154.6 (CH), 147.4 (C_q), 145.9 (C_q), 144.1 (C_q), 136.5 (C_q), 134.5 (CH), 131.8 (2 × CH), 130.6 (2 × CH), 128.9 (C_q), 127.6 (CH), 120.5 (C_q), 32.0 (CH_2), 13.3 (CH_3) ppm. EIMS (70 eV) *m/z*: 341.0 ($[M]^+$, 17), 325.9 ($[M–CH_3]^+$, 57). Elemental analysis $C_{17}H_{12}BrNO_2$: calc: C, 59.67; H, 3.53; N, 4.09; Br, 23.35. Found: C, 59.57; H, 3.65; N, 4.02; Br, 23.13.

6-(4-(Trifluoromethyl)benzyl)-7-methylquinoline-5,8-dione 2b. Yield: 51%; mp: 107–109 °C (from Et_2O). δ_H (300 MHz, $CDCl_3$, Me_4Si) 8.95 (dd, J = 4.7 Hz, 1.7 Hz, 1H), 8.36 (dd, J = 7.9 Hz, 1.7 Hz, 1H), 7.59 (dd, J = 7.9 Hz, 4.7 Hz, 1H), 7.38 ($(AB)_2$ system, J = 8.5 Hz, $\Delta\nu$ = 41.5 Hz, 4H), 4.08 (s, 2H), 2.21 (s, 3H) ppm. δ_C (75 MHz, $CDCl_3$, Me_4Si) 184.0 (C═O), 182.9 (C═O), 154.6 (CH), 147.4(C_q), 145.5(C_q), 144.3(C_q), 134.5 (CH), 129.1 (2 × CH), 127.6, (CH), 128.7 (C_q), 127.6 (CH), 125.6 (q, J = 3.8 Hz, 2 × CH); 122.2 (C_q), 32.3 (CH_2), 13.7 (CH_3) ppm. EIMS (70 eV) *m/z* : 331.0 ($[M]^+$, 41), 316.1 ($[M–CH_3]^+$, 100). Elemental analysis $C_{18}H_{12}F_3NO_2$: calc: C 65.26, H 3.65, N 4.23. Found C 65.28, H 3.71, N 4.23.

6-(3,5-Dimethoxybenzyl)-7-methylquinoline-5,8-dione 2c. Yield: 55%; mp: 110–111 °C (from Et_2O). δ_H (300 MHz, $CDCl_3$, Me_4Si) 9.02 (dd, J = 4.7 Hz, J = 1.7Hz, 1H), 8.44 (dd, J = 7.9 Hz, J = 1.7 Hz, 1H), 7.66 (dd, J = 7.8 Hz, J = 4.7 Hz, 1H), 6.41 (d, J = 2.2Hz, 2H), 6.29 (t, J = 2.2Hz, 1H), 4.04 (s, 2H), 3.75 (s, 6H), 2.33 (s, 3H) ppm. δ_C (75 MHz, $CDCl_3$, Me_4Si) 184.8 (C═O), 183.0 (C═O), 160.9 (C_q), 154.4 (CH), 147.5 (C_q), 146.0 (C_q), 144.1 (C_q), 139.7 (C_q), 134.4 (CH), 128.9 (C_q), 127.5 (CH), 107.4 (2 × CH), 98.3 (CH), 55.3 (2 × OCH_3), 32.6 (CH_2), 13.3 (CH_3) ppm. EIMS (70 eV) *m/z*: 323.2 ($[M]^+$, 42), 308.1 ($[M - CH_3]^+$, 100), 166.1 (77), 293.1 (58), 173.0 (53), 166.1 (77). Elemental analysis $C_{19}H_{17}NO_4$: calc: C, 70.58; H, 5.30; N, 4.33. Found: C, 70.30; H, 5.41; N, 4.26.

6-(2,5-Dimethoxybenzyl)-7-methylquinoline-5,8-dione 2d. Yield: 45%; mp: 135–137 °C (from Et_2O). δ_H (300 MHz, $CDCl_3$, Me_4Si) 9.02 (dd, J = 4.7 Hz, J = 1.7Hz, 1H), 8.44 (dd, J = 7.9 Hz, J = 1.7 Hz, 1H), 7.66 (dd, J = 7.8 Hz, J = 4.7 Hz, 1H), 6.80–6.70 (m, 3H), 4.08 (s, 2H), 3.80 (s, 3H), 3.73 (s, 3H), 2.80 (s, 3H) ppm. δ_C (75 MHz, $CDCl_3$, Me_4Si) 184.9 (C═O), 183.0 (C═O), 154.3 (CH), 153.6 (C_q), 151.5 (C_q), 147.8 (C_q), 146.6 (C_q), 144.4 (C_q), 134.4 (CH), 129.0 (C_q), 127.3 (CH), 127.1

(C_q), 116.5(CH), 111.6 (CH), 111.3 (CH), 56.0 (CH_3), 55.7 (CH_3), 27.1 (CH_2), 13.1 (CH_3) ppm. EIMS (70 eV) *m/z*: 323.2 ($[M]^+$, 53), 308.1($[M–CH_3]^+$, 100), 293.1 (43). Elemental analysis $C_{19}H_{17}NO_4 \cdot 0.45H_2O$: calc: C, 68.85; H 5.44; N, 4.23. Found: C, 68.25; H, 5.30; N, 4.28.

7-(4-Bromobenzyl)-3,6-dimethylquinoline-5,8-dione 3a. Yield: 57%; mp: 166–169 °C (from Et_2O). δ_H (300 MHz, $CDCl_3$, Me_4Si) 8.82 (s, 1H), 8.20 (s, 1H), 7.25 ($(AB)_2$ system, J = 8.4 Hz, $\Delta\nu$ = 87.4 Hz, 4H), 3.99 (s, 2H), 2.52 (s, 3H), 2.31 (s, 3H) ppm. δ_C (75 MHz, $CDCl_3$, Me_4Si) 184.4 (C═O), 183.5 (C═O), 155.1 (CH), 145.4 (C_q), 144.2 (C_q), 138.5 (C_q), 138.0 (C_q), 136.6 (C_q), 134.3 (CH), 131.8 (2 × CH), 130.2 (2 × CH), 128.3 (C_q), 120.5 (C_q), 31.9 (CH_2), 18.9 (CH_3), 13.5 (CH_3) ppm. EIMS (70 eV) *m/z*: 357.0 ($[M]^+$, 41), 342.0 ($[M–CH_3]^+$, 100). Elemental analysis $C_{18}H_{14}BrNO_2$: calc: C, 60.69; H, 3.96; N, 3.93; Br, 22.43. Found: C, 60.41; H, 4.15; N, 4.13; Br, 22.43.

7-(4-(Trifluoromethyl)benzyl)-3,6-dimethylquinoline-5,8-dione 3b. Yield: 45%; mp: 164–165 °C (from Et_2O). δ_H (300 MHz, $CDCl_3$, Me_4Si) 8.84 (d, J = 2.3 Hz, 1H), 8.21 (d, J = 2.3 Hz, 1H), 7.44 ($(AB)_2$ system, J = 8.1 Hz, $\Delta\nu$ = 28.2 Hz, 4H), 4.10 (s, 2H), δ = 2.52 (s, 3H), δ = 2.33 (s, 3H) ppm. δ_C (75 MHz, $CDCl_3$, Me_4Si) 184.4 (C═O), 183.5 (C═O), 155.2 (CH), 145.7 (C_q), 145.5 (C_q), 143.8 (C_q), 141.8 (C_q), 138.5 (C_q), 134.3 (CH), 128.8 (2 × CH), 128.4 (C_q), 125.6 (q, $J_{C–F}$ = 3.8 Hz, 2 × CH), 122.4 (q, $J_{C–F}$ = 272 Hz, CF_3), 32.3 (CH_2), 18.9 (CH_3), 13.6 (CH_3) ppm. EIMS (70 eV) *m/z*: 345.1 ($[M]^+$, 33), 330.0 ($[M–CH_3]^+$, 100). Elemental analysis $C_{19}H_{14}F_3NO_2$: calc: C, 66.09; H, 4.09; N, 4.06. Found: C, 65.79; H, 4.29; N, 3.86.

7-(3,5-Dimethoxybenzyl)-3,6-dimethylquinoline-5,8-dione 3c. Yield: 49%; mp: 140–141 °C (from Et_2O). δ_H (300 MHz, $CDCl_3$, Me_4Si) 8.82 (d, J = 1.7 Hz, 1H), 8.20 (d, J = 1.7 Hz, 1H), 6.36–6.30 (m, 3H), 3.98 (s, 2H), 3.75 (s, 6H), 2.51 (s, 3H), 2.32 (s, 3H) ppm. δ_C (75 MHz, $CDCl_3$, Me_4Si) 184.4 (C═O), 183.6 (C═O), 161.0 ($2C_q$), 155.0 (CH), 145.5 (C_q), 144.4 (C_q), 139.8 (C_q), 140.1 (C_q), 138.4 (C_q), 134.4 (CH), 128.4 (C_q), 106.8 (2CH), 98.1 (CH), 55.3 ($2CH_3$), 32.5 (CH_2), 18.8 (CH_3), 13.5 (CH_3) ppm. EIMS (70 eV) *m/z*: 337.1 ($[M]^+$, 80), 322.1 ($[M–CH_3]^+$, 100). Elemental analysis $C_{20}H_{19}NO_4$: calc: C, 71.20; H, 5.68; N, 4.15. Found: C, 70.88; H, 5.66; N, 4.14.

7-(2,5-Dimethoxybenzyl)-3,6-dimethylquinoline-5,8-dione 3d. Yield: 41%; mp: 129–130 °C (from Et_2O). δ_H (300 MHz, $CDCl_3$, Me_4Si) 8.83 (s, 1H), 8.20 (s, 1H), 6.78–6.62 (m, 3H), 3.79 (s, 3H), 3.71 (s, 3H), 2.51 (s, 3H), 2.24 (s, 3H) ppm. δ_C (75 MHz, $CDCl_3$, Me_4Si) 184.3 (C═O), 183.7 (C═O), 154.8 (CH), 153.5 (C_q), 151.5 (C_q), 145.8 (C_q), 145.5 (C_q), 144.9 (C_q), 138.3 (C_q), 134.4 (CH), 128.6 (C_q), 127.2 (C_q), 116.3 (CH), 111.2 (CH), 111.1 (CH), 55.9 (CH_3), 55.6 (CH_3), 26.9 (CH_2), 18.9 (CH_3), 13.2 (CH_3) ppm. EIMS (70 eV) *m/z*: 337.1 ($[M]^+$, 100); 322.1 ($[M–CH_3]^+$, 63). Elemental analysis $C_{20}H_{19}NO_4$: calc: C, 71.20; H, 5.68; N, 4.1. Found: C, 70.61; H, 5.70; N, 4.16.

6-(4-Bromobenzyl)-3,7-dimethylquinoline-5,8-dione 4a. Yield: 50%; mp: 146–148 °C (from Et_2O). δ_H (300 MHz, $CDCl_3$, Me_4Si) 8.83 (d, J = 2.0 Hz, 1H), 8.20 (d, J = 2.0 Hz, 1H), 7.26 ($(AB)_2$ system, J = 8.0 Hz, $\Delta\nu$ = 72.4 Hz, 4H), 4.04 (s, 2H), 2.52 (s, 3H), 2.26 (s, 3H) ppm. δ_C (75 MHz, $CDCl_3$, Me_4Si) 185.0 (C═O), 182.9 (C═O), 155.1 (CH), 145.7 (C_q), 145.3 (C_q), 143.8 (C_q), 138.5 (C_q), 136.6 (C_q), 134.2 (CH), 131.7 (2 × CH), 130.5 (2 × CH), 128.5 (C_q), 120.4 (C_q), 31.9 (CH_2), 18.9 (CH_3), 13.2 (CH_3) ppm. EIMS (70 eV) *m/z*: 357.0 ($[M]^+$, 35), 342.0 ($[M–CH_3]^+$, 46, 340.0, (100). Elemental analysis $C_{18}H_{14}BrNO_2$: calc: C, 60.69; H, 3.96; N, 3.93; Br, 22.43. Found: C, 60.92; H, 4.02; N, 3.89; Br, 22.28.

6-(4-(Trifluoromethyl)benzyl)-3,7-dimethylquinoline-5,8-dione 4b. Yield: 52%; mp: 121–123 °C (from Et_2O). δ_H (300 MHz, $CDCl_3$, Me_4Si) 8.83 (s, 1H), 8.21 (s, 1H), 7.45 ($(AB)_2$ system, J = 7.8 Hz, $\Delta\nu$ = 41.9 Hz), 4.14 (s, 2H), 2.52 (s, 3H), 2.27 (s, 3H) ppm. δ_C (75 MHz, $CDCl_3$, Me_4Si) 184.9 (C═O), 182.9 (C═O), 155.2 (CH), 145.3 (C_q), 145.2 (C_q), 141.7 (C_q), 143.2 (CH), 138.6 (C_q), 129.1 (2 × CH), 128.9 (q, $J_{C–F}$ = 25.6 Hz, C_q), 128.5 (C_q), 125.6 (q, $J_{C–F}$ = 3.7 Hz, 2 × CH), 124.0 (q, $J_{C–F}$ = 272.6 Hz, C_q), 32.3 (CH_2), 18.9 (CH_3), 13.3 (CH_3) ppm. EIMS (70 eV) *m/z*: 345.0 ($[M]^+$, 41), 330.0 ($[M–CH_3]^+$, 100). Elemental analysis $C_{19}H_{14}F_3NO_2$: calc: C, 66.09; H, 4.09; F, 16.51; N, 4.06. Found: C, 66.15; H, 4.12; N, 4.08.

6-(3,5-Dimethoxybenzyl)-3,7-dimethylquinoline-5,8-dione 4c. Yield: 37%; mp: 106–108 °C (from Et_2O). δ_H (300 MHz, $CDCl_3$, Me_4Si) 8.83 (d, J = 2.1 Hz, 1H), 8.20 (d, J = 2.1 Hz, 1H), 6.41–6.29 (m, 3H), 4.03 (s, 2H), 3.74 (s, 6H), 2.52 (s, 3H), 2.27 (s, 3H) ppm. δ_C (75 MHz, $CDCl_3$, Me_4Si) 185.1 (C═O), 182.9 (C═O), 160.9 (C_q), 155.0 (CH), 145.9 (C_q), 145.3 (C_q), 143.9 (C_q), 139.8 (C_q), 138.4 (C_q), 134.2 (CH), 128.5 (CH), 107.0 (C_q), 98.3 (C_q), 32.5 (CH_2), 18.8 (CH_3), 13.2 (CH_3) ppm. EIMS (70 eV) *m/z*: 337.0 ($[M]^+$, 41), 322.0 ($[M–CH_3]^+$, 100). Elemental analysis $C_{20}H_{19}NO_4$: calc: C, 71.20; H, 5.68; N, 4.15. Found: C, 70.85; H, 5.70.

6-(2,5-Dimethoxybenzyl)-3,7-dimethylquinoline-5,8-dione 4d. Yield: 58%; mp: 133–135 °C (from Et_2O). δ_H (300 MHz, $CDCl_3$, Me_4Si) 8.81 (d, J = 2.1 Hz, 1H), 8.18 (d, J = 2.1 Hz, 1H), 6.77–6.66 (m, 3H), 4.05 (s, 2H), 3.78 (s, 3H), 3.70 (s, 3H), 2.51 (s, 3H), 2.18 (s, 3H) ppm. δ_C (75 MHz, $CDCl_3$, Me_4Si) 184.3 (C═O), 183.7 (C═O), 154.8 (CH), 153.5 (C_q), 151.5 (C_q), 145.8 (C_q), 145.5 (C_q), 144.9 (C_q), 138.3 (C_q), 134.4 (CH), 128.6 (C_q), 127.2 (C_q), 116.3 (CH), 111.2 (CH), 111.1 (CH), 55.9 (CH_3), 55.6 (CH_3), 26.9 (CH_2), 18.9 (CH_3), 13.2 (CH_3) ppm. EIMS (70 eV) *m/z*: 337.13 ($[M]^+$, 65), 322.1 ($[M–CH_3]^+$, 100). Elemental analysis $C_{20}H_{19}NO_4$: calc: C, 71.20; H, 5.68; N, 4.15. Found: C, 71.35; H, 5.75; N, 4.20.

2-Methyl-3-(pyridin-4-ylmethyl)naphthalene-1,4-dione 11. 4-Pyridylacetic acid hydrochloride (2.00 g, 11.52 mmol) was dissolved in 20 mL water and stirred at rt for 5 min. Then $AgNO_3$ (2.35 g, 13.82 mmol, 1.2 equiv) was added under stirring and a white precipitate appeared in the solution. The precipitate turns black if left under light (AgCl). The precipitate was filtered and the filtrate containing the pyridinium salt was used directly in Jacobsen–Torssell reaction with menadione as reaction partner according to the reported general procedure.[2a] The residue was dissolved in CH_2Cl_2 and extracted with K_2CO_3 saturated solution. The organic phase was evaporated to produce a brown oil (200 mg). The brown oil was purified through flash chromatography with the toluene–Et_2O system (1 : 1) after a prior treatment of the column with Et_3N. The obtained powder

was recrystallized in 5 mL cyclohexane–EtOAc (10 : 1) to afford the wished compound **11** as orange crystals. Yield: 10%; mp: 120–122 °C (from cyclohexane–EtOAc). δ_H (300 MHz, $CDCl_3$, Me_4Si) 8.47–8.49 (m, 2H), 8.07–8.11 (m, 2H), 7.69–7.74 (m, 2H), 7.14–7.15 (m, 2H), 4.02 (s, 2H, CH_2), 2.23 (s, 3H, CH_3). δ_C (75 MHz, $CDCl_3$, Me_4Si) 184.9 (C═O), 184.3 (C═O), 150.0 (CH, 2C), 147.2 (C_q), 145.2 (C_q), 143.6 (C_q), 133.8 (CH), 133.7 (CH), 132.0 (C_q), 131.8 (C_q), 126.6 (CH), 126.4 (CH), 123.8 (CH, 2C), 31.9 (CH_2), 13.4 (CH_3). EIMS (70 eV) *m/z*: 263.1 ($[M]^+$, 33), 248.1 ($[M–CH_3]^+$, 100). Elemental analysis $C_{17}H_{13}NO_2$: calc: C, 77.55; H, 4.98; N, 5.32. Found: C, 77.48; H, 4.98; N, 5.30.

Cyclic voltammetry

Cyclic voltammetry measurements were carried out at 20 °C using platinum working and auxiliary electrodes (CTV 101T and platinum wire, respectively) and a potentiostat (VoltaLab Radiometer Analytical with PGZ 301). The standard calomel reference electrodes were separated from the bulk of the solution by a KCl saturated solution with a glass frit. The compounds (1 mM) were analyzed in CH_2Cl_2 solvent using tetrabutylammonium tetrafluoroborate salt (0.1 M) as supporting electrolyte. Prior to the measurements the mixtures were deoxygenated by means of a stream of dry nitrogen which was maintained above the solutions during measurements. The sweep rate was 0.2 V s^{-1}. I_{pc} and I_{pa} values are respectively the current intensities (μA) for cathodic and anodic peaks. The standard redox potentials ($E°$) were determined from cyclic voltammograms by averaging the cathodic (E_{pc}) and the anodic (E_{pa}) peak potentials. The separation of these peak potentials (ΔE_p) can be used to estimate the kinetic reversibility of the respective redox reaction. Menadione **2** and methylene blue (MB) were used as reference compounds. The results are given with reference to the Standard Calomel Electrode (SCE) potential.

Parasitology

***In vitro* assays with *Plasmodium falciparum* strains in culture.** The chloroquine-sensitive 3D7 and the multi-resistant Dd2 strains of *Plasmodium falciparum* were cultivated using standard protocols previously reported.[2,32c]

Determination of IC_{50} values against *P. falciparum* strains. Drug susceptibility of *P. falciparum* was studied using a modified method[50a] of the protocol described previously for the ^{3}H-hypoxanthine incorporation-based assay.[50b] All assays included CQ diphosphate (Sigma, UK) as standard and control wells with untreated infected and uninfected erythrocytes. IC_{50} values were derived by sigmoidal regression analysis (Microsoft xlfit™). All data from *in vitro* tests were carried out in triplicate and were given with the 95% confidence limits.

Assays with *ex vivo* Schistosoma worms. Adult *S. mansoni* worms were obtained from mice 49 days post infection by perfusion with RPMI 1640 media as described.[51] Compounds were dissolved in dimethylsulfoxide (DMSO) and added to freshly perfused worms in RPMI 1640 containing 25 mM HEPES, pH 7, 150 units mL^{-1} penicillin, 125 μg mL^{-1} streptomycin, and 10% heat-inactivated fetal calf serum (Cellgro, Mediatech). Control worms were treated with equal volumes of DMSO alone. Worms were subsequently observed for motility and mortality. Mortality was scored as a complete lack of movement. Collection of human red blood cells (RBCs) was as follows. Whole human blood was collected in a 10 mL heparinized tube (BD vacutainer, 367874). The samples were centrifuged at 400 × g for 10 min without a brake. The plasma (the upper layer) and white blood cells (interface) were removed. A volume of RPMI medium equal to that of the whole blood was added to the RBC pellet and mixed thoroughly. The samples were centrifuged at 400 g for 10 min without a brake. The wash was repeated three more times. After the final wash the upper layer was removed and the same volume of RPMI was added to the red blood cells and then mixed thoroughly. The washed RBCs were stored at 4 °C.

Physico-biochemical studies

Materials and methods. Distilled water was purified by passing it through a mixed bed of ion-exchanger (Bioblock Scientific R3-83002, M3-83006) and activated carbon (Bioblock Scientific ORC-83005). All stock solutions were prepared using an AG 245 Mettler Toledo analytical balance. The $[Fe^{III}PPIX]_{tot}$ and $[metHb(Fe^{III})]_{tot}$ were calculated from the molecular weight of the corresponding monomers. HEPES (2-[4-(2-hydroxyethyl) piperazin-1-yl]ethanesulfonic acid, Gerbu Biotechnik) buffer (0.2 m) was prepared in water and the pH (7.4) was adjusted with NaOH slurry. pH reading was done on a PHM240 MeterLab® millivoltmeter fitted with a combined glass electrode (Metrohm 6.0234.500, Long Life, 0.1 m NaCl). Calibration was done with commercial Merck® buffers (1.68, 4.00, 6.86, 7.41, and 9.18). Stock solutions of the substrates in DMSO for the different assays were freshly prepared in Eppendorf tubes just before the experiments. Hematin ($Fe^{III}PPIX(OH)$) solution was prepared from equine hemin Type III ($Fe^{III}PPIXCl$, Sigma-Aldrich) and 0.1 m NaOH solution vigorously stirred at room temperature (rt) for 1 h. Methemoglobin was prepared by oxidation of human hemoglobin (Sigma-Aldrich) in solution by oxygen at rt (the molecular weight of the tetrameric hemoglobin is 64.458 kDa). NADPH (Biomol, Hamburg, Germany) solution was prepared in water and kept at 0 °C during the experiments. Final concentration in the optical cell was calculated from the absorbance at 340 nm (ε_{340} = 6.22 mM^{-1} cm^{-1}).

Spectrophotometric titration of hematin π–π dimer by the substrates. An aliquot of 10 μL of the $Fe^{III}PPIX(OH)$ stock solution (~1.68 mm) was dissolved in 500 μl 0.2 M sodium HEPES buffer at pH 7.5 in a 1 cm Hellma optical cell. The absorption spectrophotometric titrations were carried out by adding microvolumes of a stock solution of the substrate (~5 × 10^{-4} M in DMSO). Aliquots of 5–20 μL of the stock substrate solution were successively added to the reaction mixture and, after each addition, a UV-visible absorption spectrum (300 nm < λ < 800 nm) was recorded with a Uvikon 941 spectrophotometer. Special care was taken to ensure that equilibrium was attained. The association constants K_A and the stoichiometries of the species at equilibrium were determined by processing the spectrophotometric data with the Specfit program.[52] Specfit uses

factor analysis to reduce the absorbance matrix and to extract the eigenvalues prior to the multi-wavelength fit of the reduced data set according to the Marquardt algorithm. The uncertainties on the log K values are given as 3σ with σ = standard deviation. Origin 5.0 was used to process the analytical results. For the sake of simplicity, charges are omitted in all the chemical equilibria.

β-Hematin inhibition assay. The β-hematin inhibition assay used in this work was inspired from that developed by the group of T. J. Egan[42] with some significant improvements in the order of the addition of the reactants, which were imposed by the low solubility of some of our compounds.[41b,b] Briefly, drug solutions (89.1 mM, 53.5 mM, 26.7 mM, 17.8 mM, 13.4 mM, 8.9 mM, 4.5 mM, 0 mM) were prepared by dissolving the drug in DMSO. Hematin stock solution (1.68 mM) was prepared by dissolving equine hemin (1.05 mg) in 0.1 M NaOH (960 μL). The solution was incubated at room temperature for 1 h. In a series of 2 mL Eppendorf tubes, 2.0 μL of drug solution (or solvent for the blank reference) were dispensed. Then 20.2 μL of hematin stock solution were added. The Eppendorf tubes were placed in an incubator at 60 °C and then, 2 μL of 1 M HCl and 11.7 μL of 12.9 M sodium acetate solution (pH 4.5) pre-incubated at 60 °C were added. Final hematin concentration was 1 mM. Final drug concentrations were 4.96 mM, 2.98 mM, 1.45 mM, 0.99 mM, 0.75 mM, 0.5 mM, 0.25 mM and 0 mM and final pH of the solution was 4.5. The reaction mixtures were incubated at 60 °C for 1 h. After incubation, the reaction mixtures were quenched at room temperature by adding 900 μL of 0.2 M sodium HEPES buffer + 5% (v/v) pyridine (pH 8.2) in order to adjust final pH of the mixture to a value between 7.2 and 7.5. Then 1100 μL of 0.02 M sodium HEPES buffer + 5% pyridine (v/v) (pH 7.5) was added. The Eppendorf tubes were shaken and the precipitate of β-hematin was scrapped from the walls of the Eppendorf tubes to ensure complete dissolution of hematin. The β-hematin was allowed to settle at room temperature for 1 h. The supernatant was carefully transferred to a Hellma optical cell (l = 1 cm) without disturbing the precipitate and the absorption spectra were measured between 300 and 750 nm.

Methemoglobin reduction coupled assay with hGR/NADPH. Stock solutions of 2 mM of the drugs in DMSO were freshly prepared. Solutions of 397 μM methemoglobin in *h*GR buffer and *ca.* 4 mM NADPH in water were prepared and kept at 0 °C during the experiment. Final NADPH concentration in the optical cell was calculated from the absorbance at 340 nm (ε_{340} = 6.22 mm^{-1} cm^{-1}). In a Hellma optical cell (l = 1 cm), 945 μL of the *h*GR buffer, 20 μL of the methemoglobin solution (397 μM), 20 μL of the drug solution (2 mM) and 10 μL of the NADPH solution (*ca*. 4 mM) were introduced and pre-incubated at 37.5 °C (Lauda E200/O11 thermostat and a Huber Minichiller cooler) for 5 min. Then 5 μL of the *h*GR stock II solution was added. The reaction was monitored by UV-vis. absorption spectrophotometry on a Cary 300 spectrophotometer with the scanning kinetics method. A spectrum was measured every 30 s between 250 and 500 nm over 1 to 2 h. The kinetic data were processed with the Specfit program as reported previously.[43b]

Acknowledgements

This work was funded by US NIH/National Institute of Allergy and Infectious Disease (NIAID) (grant R01AI065622). L. J. and D. A. L. are grateful to NIH (L. J., 1st year; D. A. L., 3 years) and DFG *via* the SFB 544 (B14 project) for their salaries. K.B. wishes to thank the DFG for supporting the project (BE1540-15-1). The Centre National de la Recherche Scientifique (CNRS), the University of Strasbourg (UMR 7509 CNRS-UdS), and the International Center for Frontier Research in Chemistry (ic-FRC) in Strasbourg also partly supported this work. The LC-MS analyses were performed at the TechMed^{ILL} Platform of the Unité Mixte de Service CNRS-Université de Strasbourg (UMS 3286); the authors are grateful to Patrick Gizzi for the data and the fruitful discussions. E.D.C is grateful to Prof Louis Maes, Antwerp University for the primary cytotoxicity assays with the human MRC-5 cell line. Schistosome materials for this work were supplied in part through NIH/NIAID contract HHSN272201000005I to Dr Fred Lewis at the Biomedical Research Institute, Rockville, MD, USA.

Notes and references

1 A. G. Ross, P. B. Bartley, A. C. Sleigh, G. R. Olds, Y. Li, G. M. Williams and D. P. McManus, *N. Engl. J. Med.*, 2002, **346**, 1212.
2 (*a*) T. Müller, L. Johann, B. Jannack, M. Brückner, D. A. Lanfranchi, H. Bauer, C. Sanchez, V. Yardley, C. Deregnaucourt, J. Schrevel, M. Lanzer, R. H. Schirmer and E. Davioud-Charvet, *J. Am. Chem. Soc.*, 2011, **133**, 11557; (*b*) E. Davioud-Charvet and D. A. Lanfranchi, in Apicomplexan parasites Molecular approaches toward targeted drug development. *Drug Discovery in Infectious Diseases*, ed. K. Becker, P. M. Selzer, Wiley-VCH, Weinheim, 2011, vol. 2.
3 T. Hogg, K. Nagarajan, S. Herzberg, L. Chen, X. Shen, H. Jiang, M. Wecke, C. Blohmke, R. Hilgenfeld and C. L. Schmidt, *J. Biol. Chem.*, 2006, **281**, 25425.
4 (*a*) T. J. Egan, *Mini-Rev. Med. Chem.*, 2001, **1**, 113; (*b*) P. M. O'Neill, S. A. Ward, N. G. Berry, J. P. Jeyadevan, G. A. Biagini, E. Asadollaly, B. K. Park and P. G. Bray, *Curr. Top. Med. Chem.*, 2006, **6**, 479; (*c*) B. L. Tekwani and L. A. Walker, *Curr. Opin. Infect. Dis.*, 2006, **19**, 623.
5 (*a*) W. S. Marsh, A. L. Garretson and E. M. Wesel, *Antibiot. Chemother.*, 1961, **11**, 151; (*b*) T. J. McBride, J. J. Oleson and D. Woolf, *Cancer Res.*, 1966, **26**, 727; (*c*) J. W. Lown and S. K. Sim, *Can. J. Biochem.*, 1976, **54**, 446; (*d*) I. A. Shaikh, F. Johnson and A. P. Grollman, *J. Med. Chem.*, 1986, **29**, 1329; (*e*) M. S. Cohen, Y. Chai, B. E. Britigan, W. McKenna, J. Adams, T. Svendsen, K. Bean, D. Hassett and P. F. Sparling, *Antimicrob. Agents Chemother.*, 1987, **31**, 1507; (*f*) M. N. Preobrazhenskaya, N. V. Holpne-Kozlova and E. I. Lazhko, *J. Antibiot.*, 1992, **45**, 227; (*g*) A. D. Bolzan and M. S. Bianchi, *Mutat. Res.*, 2001, **488**, 25; (*h*) G. Bringmann, Y. Reichert and V. V. Kane, *Tetrahedron*, 2004, **60**, 3539.
6 (*a*) D. L. Boger, M. Yasuda, L. A. Mitscher, S. D. Drake, P. A. Kitos and S. C. Thompson, *J. Med. Chem.*, 1987, **30**, 1918; (*b*) M. Hassani, W. Cai, D. C. Holley, J. P. Lineswala, B. R. Maharjan, G. R. Ebrahimian, H. Seradj, M. G. Stocksdale, F. Mohammadi, C. C. Marvin, J. M. Gerdes, H. D. Beall and M. Behforouz, *J. Med. Chem.*, 2005, **48**, 7733; (*c*) M. Hassani, W. Cai, K. H. Koelsch, D. C. Holley, A. S. Rose, F. Olang, J. P. Lineswala, W. G. Holloway, J. M. Gerdes, M. Behforouz and H. D. Beall, *J. Med. Chem.*, 2008, **51**, 3104.
7 A. du Moulinet d'Hardemare, G. Serratrice and J. L. Pierre, *BioMetals*, 2004, **17**, 691.
8 C. Morin, T. Besset, J. Moutet, M. Fayolle, M. Brueckner, D. Limosin, K. Becker and E. Davioud-Charvet, *Org. Biomol. Chem.*, 2008, **6**, 2731 and references cited therein for redox potential values following one to two nitrogen introduction.
9 (*a*) T. Y. Matrosovich, F. I. Lobanov and N. V. Mahanov, *Zh. Neorg. Khim.*, 1986, **31**, 1441; (*b*) T. Turnquist and E. Sandell, *Anal. Chim. Acta*, 1968, **42**, 239; (*c*) W. Q. Ding and S. E. Lind, *IUBMB Life*, 2009, **61**, 1013; (*d*) M. Albrecht, M. Fiege and O. Osetska, *Coord. Chem. Rev.*,

2008, **252**, 812; (*e*) H. N. Yeowell and J. R. White, *Antimicrob. Agents Chemother.*, 1982, **22**, 961.
10 (*a*) L. W. Scheibel and A. Adler, *Mol. Pharmacol.*, 1981, **20**, 218–223 and 1982, **22**, 140 (*b*) L. W. Scheibel, *Prog. Clin. Biol. Res.*, 1984, **165**, 377; (*c*) L. W. Scheibel and G. G. Stanton, *Mol. Pharmacol.*, 1986, **30**, 364; (*d*) L. W. Scheibel and S. Rodriguez, *Prog. Clin. Biol. Res.*, 1989, **313**, 119.
11 D. R. Richardson, *Expert Opin. Invest. Drugs*, 1999, **8**, 2141.
12 N. Jacobsen and K. Torssell, *Acta Chem. Scand.*, 1973, **27**, 3211.
13 J. K. Kochi and J. M. Anderson, *J. Am. Chem. Soc.*, 1970, **92**, 1651.
14 V. Petrow and B. Sturgeon, *J. Chem. Soc.*, 1954, 570.
15 R. Barret and M. Daudon, *Tetrahedron Lett.*, 1990, **31**, 4871.
16 S. Hibino and S. M. Weinreb, *J. Org. Chem.*, 1977, **42**, 232.
17 H. M. Van Dort and H. J. Geursen, *Recl. Trav. Chim. Pays-Bas*, 1967, **86**, 520.
18 J. Cossy and D. Belotti, *Tetrahedron Lett.*, 2001, **42**, 4329.
19 D. W. Kim, H. Y. Choi, K.-J. Lee and D. Y. Chi, *Org. Lett.*, 2001, **3**, 445.
20 K. Sachin, H.-J. Jeong, S. T. Lim, M.-H. Sohn, D. Y. Chi and D. W. Kim, *Tetrahedron*, 2011, **67**, 1763.
21 M. Behforouz and M. Ahmadian, *Tetrahedron*, 2000, **56**, 5259.
22 (*a*) B. S. Poncin, A.-M. H. Frisque and L. Ghosez, *Tetrahedron Lett.*, 1982, **23**, 3261; (*b*) D. L. Boger, *Tetrahedron*, 1983, **39**, 2869.
23 A. Díaz-Ortiz, J. R. Carrillo, F. P. Cossío, M. J. Gómez-Escalonilla, A. de la Hoz, A. Moreno and P. Prieto, *Tetrahedron*, 2000, **56**, 1561.
24 P. Benezeth, D. Palmer and D. Wesolowski, *J. Chem. Eng. Data*, 2001, **46**, 202.
25 M. Chigr, H. Fillion and A. Rougny, *Tetrahedron Lett.*, 1988, **29**, 5913.
26 L. Salmon-Chemin, E. Buisine, V. Yardley, S. Kohler, M. A. Debreu, V. Landry, C. Sergheraert, S. L. Croft, R. L. Krauth-Siegel and E. Davioud-Charvet, *J. Med. Chem.*, 2001, **44**, 548.
27 F. Minisci, *Synthesis*, 1973, 1–24.
28 (*a*) M. F. Oliveira, J. C. d'Avila, C. R. Torres, P. L. Oliveira, A. J. Tempone, F. D. Rumjanek, C. M. Braga, J. R. Silva, M. Dansa-Petretski, M. A. Oliveira, W. de Souza and S. T. Ferreira, *Mol. Biochem. Parasitol.*, 2000, **111**, 217; (*b*) M. M. Chen, L. Shi and D. J. Sullivan Jr, *Mol. Biochem. Parasitol.*, 2001, **113**, 1.
29 (*a*) J. B. Corrêa Soares, C. M. Maya-Monteiro, P. R. Bittencourt-Cunha, G. C. Atella, F. A. Lara, J. C. d'Avila, D. Menezes, M. A. Vannier-Santos, P. L. Oliveira, T. J. Egan and M. F. Oliveira, *FEBS Lett.*, 2007, **581**, 1742; (*b*) T. J. Egan, *J. Inorg. Biochem.*, 2008, **102**, 1288; (*c*) J. B. Corrêa Soares, D. Menezes, M. A. Vannier-Santos, A. Ferreira-Pereira, G. T. Almeida, T. M. Venancio, S. Verjovski-Almeida, V. K. Zishiri, D. Kuter, R. Hunter, T. J. Egan and M. F. Oliveira, *PLoS Negl. Trop. Dis.*, 2009, **3**, e477.
30 (*a*) T. J. Egan, *J. Inorg. Biochem.*, 2008, **102**, 1288; (*b*) T. J. Egan, *Mol. Biochem. Parasitol.*, 2008, **157**, 127; (*c*) I. Weissbuch and L. Leiserowitz, *Chem. Rev.*, 2008, **108**, 4899; (*d*) C. Asher, K. A. de Villiers and T. J. Egan, *Inorg. Chem.*, 2009, **48**, 7994.
31 (*a*) H. M. Alger and D. L. Williams, *Mol. Biochem. Parasitol.*, 2002, **121**, 129; (*b*) A. N. Kuntz, E. Davioud-Charvet, J. Dessolin, A. A. Sayed, L. L. Califf, E. S. J. Arnér and D. L. Williams, *PLoS Med.*, 2007, **4**, e206, 1. Erratum in *PLoS Med*., 2007, **4**, e264.
32 (*a*) C. Biot, H. Bauer, R. H. Schirmer and E. Davioud-Charvet, *J. Med. Chem.*, 2004, **47**, 5972; (*b*) H. Bauer, K. Fritz-Wolf, A. Winzer, S. Kühner, S. Little, V. Yardley, H. Vezin, B. Palfey, H. Schirmer and E. Davioud-Charvet, *J. Am. Chem. Soc.*, 2006, **128**, 10784; (*c*) W. Friebolin, B. Jannack, N. Wenzel, J. Furrer, T. Oeser, C. P. Sanchez, M. Lanzer, V. Yardley, K. Becker and E. Davioud-Charvet, *J. Med. Chem.*, 2008, **51**, 1260.
33 (*a*) K. Blumenstiel, R. Schöneck, V. Yardley, S. L. Croft and R. L. Krauth-Siegel, *Biochem. Pharmacol.*, 1999, **58**, 1791; (*b*) E. I. Ramos, K. M. Garza, R. L. Krauth-Siegel, J. Bader, L. E. Martinez and R. A. Maldonado, *J. Parasitol.*, 2009, **95**, 461.
34 P. Loria, S. Miller, M. Foley and L. Tilley, *Biochem. J.*, 1999, **339**, 363.
35 (*a*) R. H. Schirmer, J. G. Müller and R. L. Krauth-Siegel, *Angew. Chem., Int. Ed. Engl.*, 1995, **34**, 141; (*b*) R. L. Krauth-Siegel, H. Bauer and R. H. Schirmer, *Angew. Chem., Int. Ed.*, 2005, **44**, 690.
36 (*a*) H. Atamna and H. Ginsburg, *J. Biol. Chem.*, 1995, **270**, 24876; (*b*) S. Meierjohan, R. D. Walter and S. Müller, *Biochem. J.*, 2002, **368**, 761.
37 M. F. Oliveira, J. C. d'Avila, A. J. Tempone, J. B. Soares, F. D. Rumjanek, A. Ferreira-Pereira, S. T. Ferreira and P. L. Oliveira, *J. Infect. Dis.*, 2004, **190**, 843.
38 K. A. de Villiers, H. M. Marques and T. J. Egan, *J. Inorg. Biochem.*, 2008, **102**, 1660.
39 (*a*) S. H. Xiao and B. A. Catto, *Antimicrob. Agents Chemother.*, 1989, **33**, 1557; (*b*) Y. L. Hong, Y. Z. Yang and S. R. Meshnick, *Mol. Biochem. Parasitol.*, 1994, **63**, 121; (*c*) D. L. Klayman, *Science*, 1985, **228**, 1049.
40 (*a*) J. Xu Kelly, R. Winter, M. Riscoe and D. H. Peyton, *J. Inorg. Biochem.*, 2001, **86**, 617; (*b*) I. Nabih, *J. Pharm. Sci.*, 1966, **55**, 221; (*c*) M. V. Ignatushchenko, R. W. Winter, H. P. Bächinger, D. J. Hinrichs and M. K. Riscoe, *FEBS Lett.*, 1997, **409**, 67; (*d*) M. Riscoe, J. X. Kelly and R. Winter, *Curr. Med. Chem.*, 2005, **12**, 2539.
41 (*a*) O. Blank, E. Davioud-Charvet and M. Elhabiri, *Antioxid. Redox Signaling*, 2012, **17**, 544; (*b*) L. Johann, E. Davioud-Charvet, D. A. Lanfranchi and M. Elhabiri, *Curr. Pharm. Des.*, 2012, **18**, 3539, and references cited therein for protocols of physico-(bio)chemical assays..
42 K. K. Ncokazi and T. J. Egan, *Anal. Biochem.*, 2005, **338**, 306–319.
43 (*a*) S. Partos, *Biochem. Z.*, 1922, **129**, 89; (*b*) H. M. Marques, O. Q. Munro and M. L. Crawcour, *Inorg. Chim. Acta*, 1992, **196**, 221.
44 (*a*) P. M. Färber, L. D. Arscott, C. H. Williams Jr, K. Becker and R. H. Schirmer, *FEBS Lett.*, 1998, **422**, 311; (*b*) K. Buchholz, R. H. Schirmer, J. K. Eubel, M. B. Akoachere, T. Dandekar, K. Becker and S. Gromer, *Antimicrob. Agents Chemother.*, 2008, **52**, 183.
45 C. A. Lipinski, F. Lombardo, B. W. Dominy and P. J. Feeney, *Adv. Drug Delivery Rev.*, 2001, **46**, 3.
46 (*a*) K. Buchholz, E. D. Putrianti, S. Rahlfs, R. H. Schirmer, K. Becker and K. Matuschewski, *J. Biol. Chem.*, 2010, **285**, 37388; (*b*) R. Pastrana-Mena, R. R. Dinglasan, B. Franke-Fayard, J. Vega-Rodríguez, M. Fuentes-Caraballo, A. Baerga-Ortiz, I. Coppens, M. Jacobs-Lorena, C. J. Janse and A. E. Serrano, *J. Biol. Chem.*, 2010, **285**, 27045.
47 S. M. Kanzok, A. Fechner, H. Bauer, J. K. Ulschmid, H. M. Müller, J. Botella-Munoz, S. Schneuwly, R. H. Schirmer and K. Becker, *Science*, 2001, **291**, 643.
48 (*a*) L. Luzzatto, *Experientia*, 1995, **51**, 206; (*b*) C. Ruwende and A. Hill, *J. Mol. Med.*, 1998, **76**, 581; (*c*) M. Aidoo, D. J. Terlouw, M. S. Kolczak, P. D. McElroy, F. O. ter Kuile, S. Kariuki, B. L. Nahlen, A. A. Lal and V. Udhayakumar, *Lancet*, 2002, **359**, 1311; (*d*) M. D. Cappellini and G. Fiorelli, *Lancet*, 2008, **371**, 64.
49 (*a*) K. Ayi, F. Turrini, A. Piga and P. Arese, *Blood*, 2004, **104**, 3364; (*b*) M. Cappadoro, G. Giribaldi, E. O'Brien, F. Turrini, F. Mannu, D. Ulliers, G. Simula, L. Luzzatto and P. Arese, *Blood*, 1998, **92**, 2527; (*c*) V. Gallo, E. Schwarzer, S. Rahlfs, R. H. Schirmer, R. van Zwieten, D. Roos, P. Arese and K. Becker, *PLoS One*, 2009, **4**, e7303.
50 (*a*) A. Cameron, J. Read, R. Tranter, V. J. Winter, R. B. Sessions, R. L. Brady, L. Vivas, A. Easton, H. Kendrick, S. L. Croft, D. Barros, J. L. Lavandera, J. J. Martin, F. Risco, S. Garcia-Ochoa, F. J. Gamo, L. Sanz, L. Leon, J. R. Juiz, R. Gabarro, A. Mallo and F. Gomez de las Heras, *J. Biol. Chem.*, 2004, **279**, 31429; (*b*) R. E. Desjardins, C. J. Canfield, J. D. Haynes and J. D. Chulay, *Antimicrob. Agents Chemother.*, 1979, **16**, 710.
51 F. Lewis, *Schistosomiasis in Current Protocols in Immunology*, ed. J. E. Coligan, A. M. Kruisbeek, D. H. Margulies, E. M. Shevach and W. Strober, John Wiley & Sons, New York, 1998, Suppl. 28, 19.1.1–19.1.28.
52 (*a*) H. Gampp, M. Maeder, C. J. Meyer and A. D. Zuberbühler, *Talanta*, 1985, **32**, 95; (*b*) F. J. C. Rossoti, H. S. Rossoti and R. J. Whewell, *J. Inorg. Nucl. Chem.*, 1971, **33**, 2051; (*c*) H. Gampp, M. Maeder, C. J. Meye and A. D. Zuberbühler, *Talanta*, 1985, **32**, 257; (*d*) H. Gampp, M. Maeder, C. J. Meyer and A. D. Zuberbühler, *Talanta*, 1986, **33**, 943; (*e*) D. W. Marquardt, *J. Soc. Ind. Appl. Math.*, 1963, **11**, 431; (*f*) M. Maeder and A. D. Zuberbühler, *Anal. Chem.*, 1990, **62**, 2220.